

BLUE COPPER OXIDASES

A. MESSERSCHMIDT

Max-Planck-Institut für Biochemie, D-W 82 152 Martinsried, Germany

- I. Introduction
- II. Occurrence, Sequences, and Biological Function
- III. Molecular and Spectroscopic Properties
- IV. X-Ray Structure of Ascorbate Oxidase
 - A. Crystallization
 - B. Overall Description of the Structure
 - C. Secondary Structure and Tetramer Contact Surface Areas
 - D. Copper Site Geometries
- V. Structural Relationships among the Blue Copper Oxidases
 - A. Amino-Acid Sequence Alignment
 - B. Structural Model of the Copper Sites for Ceruloplasmin
- VI. Fungal Laccases, Ascorbate Oxidases, and Related Proteins
- VII. Evolution of the Blue Oxidases and Related Proteins from a Common Ancestor
- VIII. Oxidation-Reduction Potentials
- IX. Kinetic Properties of Laccase and Ascorbate Oxidase
- X. Functional Derivatives
 - A. General Remarks
 - B. X-Ray Structure of the Type-2 Depleted (T2D) Form of Ascorbate Oxidase
 - C. X-Ray Structure of the Reduced Form of Ascorbate Oxidase
 - D. X-Ray Structure of the Peroxide Form of Ascorbate Oxidase
 - E. X-Ray Structure of the Azide Form of Ascorbate Oxidase
- XI. The Catalytic Mechanism
- XII. Electron Transfer Processes
 - A. Electron Transfer to the Type-1 Copper Redox Center
 - B. Intramolecular Electron Transfer from the Type-1 Copper Center to the Trinuclear Copper Center
 - C. Electron Transfer within the Trinuclear Copper Site
- XIII. Summary
- References

I. Introduction

The activation of dioxygen in biological systems has been the focus of interest of biochemists, bioinorganic chemists, and physiologists for many years (see, for example, King *et al.* (1)). Enzymes involved in

direct oxygen activation are oxidases and oxygenases. Oxygenases introduce either one atom of dioxygen into the substrate and reduce the other atom to water (monooxygenases) or transfer two oxygen atoms into the substrate (dioxygenases). Oxidases can be divided into two-electron and four-electron transferring enzymes. The first group reduces dioxygen to hydrogen peroxide and the second one, dioxygen to water. Most of the oxygenases as well as oxidases contain as prosthetic groups flavin, iron (heme or nonheme), or copper.

Oxygen is used for respiration upon reduction to water by cytochrome c oxidase, the terminal oxidase of the respiratory chain. Cytochrome c oxidase is a complex metalloprotein containing two or three copper ions and two heme groups (a and a_3) that performs a critical function in cellular respiration in both prokaryotes and eukaryotes. The enzyme catalyzes the four-electron reduction of dioxygen with concomitant one-electron oxidation of cytochrome c. Energy released in this exergonic reaction is conserved as a pH gradient and a transmembrane potential generated in part by H^+ consumption and also by proton translocation through the protein complex (see, for example, the review on cytochrome c oxidase by Capaldi (2)).

Ascorbate oxidase, laccase, and ceruloplasmin form the group of blue oxidases. These are multicopper enzymes catalyzing the four-electron reduction of dioxygen to water with concomitant one-electron oxidation of the substrate (3), which is very similar to the reaction performed by cytochrome c oxidase. All three enzymes have been known for many years, and an overwhelming number of papers have appeared since their discovery dealing with the different aspects of these enzymes.

Laccase was discovered in 1883 by Yoshida (4), who found that the latex of the Chinese or Japanese lacquer tree rapidly hardened to a plastic in the presence of oxygen, and he attributed this to the presence of a "diastase" in the lacquer. A few years later Bertrand (5) further purified this enzyme and named it "laccase." He suggested that laccase is a metalloprotein containing manganese and introduced the term "oxidase." About 50 years later Keilin and Mann (6) demonstrated that laccase is a copper enzyme and showed that its blue color disappears reversibly upon addition of substrate. Laccase has been extensively reviewed by the researchers in this field over the last 20 years, and a representative selection is listed (3, 7-12).

Ascorbate oxidase was discovered in 1928 by Szent-Györgyi (13), who found that certain plant tissues could catalyze the aerobic oxidation of ascorbic acid, and in 1930 (14) he postulated the existence of a specific enzyme in cabbage leaves. In 1940 Lovett-Janison and Nelson (15) and Stotz (16) could confirm the existence of ascorbate oxidase and its

function as a copper-containing enzyme. Since that time this enzyme has also been investigated in detail, and the results are summarized in several reviews (17–20).

Ceruloplasmin is a plasma protein and was first isolated by Holmberg in 1944 (21). Between 1947 and 1951 Holmberg and Laurell (22) demonstrated that this α_2 -globulin was responsible for a high-affinity binding of copper in plasma. This enzyme was named "ceruloplasmin." Several comprehensive reviews (3, 7, 8, 23–29) have been published during the last three decades and include detailed biological, structural, spectroscopic, kinetic, physiological, and genetic information.

This chapter will concentrate mainly on structural and functional aspects of these enzymes with the major emphasis on ascorbate oxidase and laccase. Significant progress has been achieved in the last 10 years: the determination of amino acid sequences of all three enzymes, each from several sources, and the X-ray structure of ascorbate oxidase. The new information forms the basis of a much deeper understanding of the function of the enzymes as will be demonstrated in this chapter.

II. Occurrence, Sequences, and Biological Function

Laccase is widely distributed in plants and fungi. Laccase from higher plants, found in various species of the Chinese, Vietnamese, and Japanese lacquer trees, has been extensively investigated (9). The biological function of laccase in these trees is well understood. The laccase of the lacquer trees (*Rhus* sp.) is found in white latex, which contains phenols. After injury of the tree, these are oxidized by dioxygen to radicals, which spontaneously polymerize, building a protective structure that closes the wound.

Laccase is very abundant in fungi. Almost every basidiomycete examined contains laccase, extra- and/or intracellular at least at some stage of its development (30). Extracellular laccase appears to be present in many mycorrhizal fungi (31). Laccase is also very frequently found in ascomycetes. The best characterized fungal laccase is from the basidiomycete *Polyporus versicolor* (9). Further fungal laccases have been isolated and purified from the basidiomycetes *Phlebia radiata* (32) and *Armillaria mellea* (33), the ascomycetes *Neurospora crassa* (34, 35) and *Monocillium indicum* Saxena (36), and the chestnut blight *Cryphonectria parasitica* (37) as well as from the deuteromycete *Aspergillus nidulans* (38). The genes of the following fungal laccases have been cloned and sequenced: *N. crassa* (39), *A. nidulans* (40), *Coriolus hirsutus* (41), *P. radiata* (32), and *C. parasitica* (37).

The biological function of fungal laccase has been postulated as playing a role in sporulation (42), pigment production (43, 44), lignin degradation (45, 46), and pathogenesis (47, 48). There has been increasing interest in the ligninolytic laccase from white-rot fungi such as *P. radiata* due to their potential for industrial applications (32). In fact, *P. radiata* laccase is able to remove monomeric lignin-related compounds from residual lignin from the pulping process. Considerable progress in the industrial application of this enzyme has been achieved by Saloheimo and Niku-Paalova (49), who could generate the heterologous expression of the *P. radiata* laccase gene in the filamentous fungus *Trichoderma reesei* in larger amounts. Laccase has a low specificity with regard to the reducing substrate and oxidizes monophenols, diphenols, polyphenols, aminophenols, and diamines.

Ascorbate oxidase is found in higher plants, but cucumber, *Cucumis sativus*, and green zucchini squash, *Cucurbita pepo medullosa*, are the most common sources (19). The immunohistochemical localization of ascorbate oxidase in green zucchini reveals that ascorbate oxidase is distributed ubiquitously over vegetative and reproductive organs in all specimens examined (50). Primary structures of ascorbate oxidase from cucumber, *C. sativus* (51), pumpkin, *Cucurbita* sp. Ebisu Nankin (52), and zucchini, *C. pepo medullosa* (53), have recently been reported.

The *in vivo* role of ascorbate and ascorbate oxidase in plants is still under debate. As catechols and polyphenols are also substrates *in vitro* (54), ascorbate oxidase might be involved in processes like fruit ripening. A role in a redox system, as an alternative to the mitochondrial chain, in growth promotion, or in susceptibility to disease has also been postulated (55). It was suggested that ascorbate oxidase might be involved in reorganization of the cell wall to allow for expansion (56). This was deduced from the findings that ascorbate oxidase is highly expressed at a stage when rapid growth is occurring (in both fruits and leaves) and is localized in the fruit epidermis, where cells are under the greatest tension during rapid growth in girth.

The high catalytic activity of ascorbate oxidase toward an important biological molecule like L-ascorbate has been used for practical purposes. The main application has been the removal of ascorbate and/or oxygen from biological samples (56a) and feedstuff. Ascorbate oxidase is highly specific for the reducing substrate, ascorbate, and other compounds with an enediol group adjacent to a carbonyl group.

Ceruloplasmin is present in the plasma of all mammals examined and in birds. The amino-acid sequence of human ceruloplasmin has been determined by protein sequencing techniques (57) and later by cDNA sequencing (58). Recently, the primary structure of rat cerulo-

plasmin has been reported (59). Many functions have been ascribed to ceruloplasmin, including mobilization, transport, and homeostasis of copper, ferroxidase, amino oxidase, and possibly superoxide dismutase activity. Ceruloplasmin is an acute-phase protein in the inflammatory response (60). The protein is deficient in Wilson's disease, an autosomal recessive trait with a defect in copper metabolism (61). Ceruloplasmin catalyzes the oxidation of a great variety of both organic and inorganic substances, including amines like *p*-phenylenediamine, dopamines, and serotonin, as well as catechol derivatives, aminophenols, and Fe(II).

III. Molecular and Spectroscopic Properties

Molecular as well as spectroscopic properties of representative members of the blue copper oxidases are summarized in Tables I (62–69) and II (70–72), respectively. Data from other spectroscopic techniques used on blue oxidases, such as fluorescence, CD, or resonance Raman spectroscopy, have not been included because the implications of most of these studies are not so striking. The interested reader is referred to the existing review articles (10, 18, 19, 26).

Laccases are monomeric glycoenzymes. The molecular masses for the fungal laccases range between 59 and 65 kDa. The reported carbo-

TABLE I

MOLECULAR PROPERTIES OF REPRESENTATIVE MEMBERS OF BLUE COPPER OXIDASES

Blue copper oxidase	Amino acids	Molecular mass of protein (kDa)	Molecular mass of whole enzyme (kDa)	Carbohydrate content (%)	IP	Reference
Laccase						
Fungal						
<i>Polyporus versicolor</i>						
A	ND ^a	ND	64.4	10–14	3.1	(62, 63)
B	ND	ND	64.7	10	4.6–6.8	(62–64)
<i>Neurospora crassa</i>	ND	63.161	64	11–12	5.0–7.2	(34, 35, 39)
<i>Phlebia radiata</i>	570	56.433	64	11–12	4.9 ^b	(32, 65)
<i>Armillaria mellea</i>	527	ND	59	ND	4.1	(33)
	ND					
Tree						
<i>Rhus venicifera</i>	ND	ND	110–141	45	8.6	(66)
Ascorbate oxidase						
<i>Cucurbita pepo medullosa</i>	552	61.703	140 ^c	3	6.8 ^b	(53, 67, 68)
<i>Cucumis sativus</i>	554	62.247	132 ^c	ND	7.3 ^b	(51, 69)
Ceruloplasmin						
Human	1046	129.09	134	10	4.4	(26, 57)

^a ND, not determined.

^b Calculated from the amino-acid sequence without carbohydrate contribution.

^c The protein exists as a homodimer in solution.

TABLE II
SPECTROSCOPIC PROPERTIES OF REPRESENTATIVE BLUE COPPER OXIDASES

Blue copper oxidase	No. and type of copper center	EPR parameters				Absorption band (nm) (ϵ , $M^{-1} \text{ cm}^{-1}$)	Reference
		g_{\parallel}	g_{\perp}	$A_{\parallel} (\times 10^{-4} \text{ cm}^{-1})$			
Laccase							
Fungal							
<i>Polyporus versicolor</i> A	One type 1	2.19	2.03	90	610 (4,900)	(10)	
	One type 2	2.24	2.04	194			
	One type 3				330 (2,700)		
<i>Neurospora crassa</i>	One type 1	2.19	2.04	90	595 (3,300)	(35)	
	One type 2	2.23	2.04	185			
	One type 3				330 (2,400)		
<i>Phlebia radiata</i>	One type 1	2.19	—	90	605 (NR)	(70)	
	One type 2	2.25	—	>170			
	No type 3 ^a						
Tree							
<i>Rhus vernicifera</i>	One type 1	2.23	2.05	43	615 (5,700)	(10)	
	One type 2	2.24	2.05	200			
	One type 3				330 (2,800)		
Ascorbate oxidase							
<i>Cucurbita pepo medullosa</i>	Two type 1	2.227	2.058, 2.036	56	610 (9,700)	(67)	
	Two type 2	2.242	2.053	190			
	Two type 3				330 (3,050)		
<i>Cucumis sativus</i>	Two type 1	2.23	2.05	63	607 (10,400)	(71)	
	Two type 2	2.25	2.05	200		(72)	
	Two type 3				330 (8,600) ^b	(71)	
Ceruloplasmin							
Human	First type 1	2.215	2.06	92	610 (10,000)	(26)	
	Second type 1	2.206	2.05	72	610 (10,000)		
	Third type 1 ^c						
	One type 2	2.247	2.06	189			
	One type 3				330 (3,300)		

^a This laccase is supposed to contain only two coppers and one PQQ per mole.

^b Seems to be incorrectly estimated.

^c No distinct EPR signal observed. The nature of this type-1 copper is discussed in the text.

hydrate content is about 10%. The lengths of the published amino-acid sequences are between 500 and 600 for the mature enzymes. The isoelectric point usually lies in the acidic pH region. But the preparations of *P. versicolor* and *N. crassa* laccase consist of several isoenzymes with isoelectric points up to neutral pHs. The molecular properties of tree laccases show some differences. The molecular weights are from 110 to 140 kDa with varying carbohydrate contents. The maximum carbohydrate content has been determined to be 45%. The protein part of the enzyme was assessed to be about 65 kDa. The isoelectric point of tree laccase is in the basic pH region.

Ascorbate oxidase, also a glycoprotein, is present in solution as a

homodimer with molecular masses between 130 and 140 kDa. One monomer is built up by a single polypeptide chain of about 550 residues. The carbohydrate content of 3% is very low. The isoelectric points calculated from the amino-acid sequences without carbohydrate contribution are in the neutral pH region.

The glycoprotein ceruloplasmin is a monomeric enzyme with a molecular mass of about 130 kDa and 1000 amino-acid residues. The carbohydrate content has been determined to be 10% and an acidic isoelectric point of 4.4 for human ceruloplasmin has been reported.

The spectral properties of the blue oxidases are very similar. The copper ions of copper proteins have been classified according to their distinct spectroscopic properties (8). Type-1 Cu^{2+} shows high absorption in the visible region (ϵ generally $> 3000 \text{ M}^{-1} \text{ cm}^{-1}$ at 600 nm) and an EPR spectrum with $A_{\parallel} < 95 \times 10^{-4} \text{ cm}^{-1}$. Type-2, or normal, Cu^{2+} has undetectable absorption and the EPR line shape of the low-molecular-mass copper complexes ($A_{\parallel} > 140 \times 10^{-4} \text{ cm}^{-1}$). Type-3 (Cu^{2+}) is characterized by strong absorption in the near-ultraviolet region ($\lambda = 330 \text{ nm}$) and by the absence of an EPR signal. The type-3 center consists of a pair of copper ions that are antiferromagnetically coupled. The above-mentioned signals disappear upon reduction.

The number and type of copper centers, EPR parameters, and the two relevant absorption bands in the visible region for several representative members of the blue oxidases are listed in Table II. All laccases except that of the *P. radiata* enzyme contain four coppers per molecule with one type-1, one type-2, and one type-3 copper center. The EPR and absorption parameters resemble each other very much. *Phlebia radiata* laccase is supposed to contain only two coppers with one type 1, one type 2, and one PQQ per mole (70). This is quite unusual and will be discussed critically below, since it is possible that the copper content determined for this enzyme is inaccurate. Ascorbate oxidases have eight coppers per homodimer with two type-1, two type-2, and two type-3 copper centers. Ceruloplasmin typically contains six to seven copper ions per molecule with three type-1, one type-2, and one type-3 copper centers. It has also been proposed that there are only two type-1 copper ions and a new type-4 copper that is presumed to exhibit no EPR signal. In addition there is a variable content of chelatable copper. It is responsible for copper contents exceeding 6 coppers/mol but does not seem to be required for catalysis. It is now generally accepted that ceruloplasmin has three type-1 copper centers and the reason for this will be discussed below.

It turns out from the recently determined X-ray structure of ascorbate oxidase (73, 74) that the nonblue EPR-active type-2 copper together

with the type-3 copper pair is an integral part of a trinuclear active copper center. There has been experimental evidence in earlier studies that the type-2 copper is close to the type-3 copper and forms a trinuclear active copper site (75–80). Solomon and co-workers, based on spectroscopic studies of azide binding to tree laccase (79, 80), classified this metal binding site as a trinuclear active copper site.

IV. X-Ray Structure of Ascorbate Oxidase

A. CRYSTALLIZATION

The first crystals of a blue copper oxidase were obtained from human ceruloplasmin in 1962 (81). Since that time several successful crystallizations of ceruloplasmin from different species have been reported (26). Crystals of human native ceruloplasmin were crystallographically characterized by Magdoff-Fairchild *et al.* (82) and later by Zaytsev *et al.* (83). The crystals are tetragonal, space group $I4$, and diffract to a resolution of about 3.5 Å. The unit cell has dimensions of $a = b = 268$ Å and $c = 129$ Å and contains two molecules per asymmetric unit. Zaytsev *et al.* (84) have obtained a trigonal crystal form, space group $P3_121$ or $P3_221$ ($a = b = 214$ Å, $c = 84.5$ Å), with only one molecule per asymmetric unit, also from native human ceruloplasmin. The crystals diffract to 3.5 Å resolution in contrast to an isomorphous trigonal form from asialoceruloplasmin (83), which diffract only to 6.0 Å. This crystal form therefore seems to be very promising for X-ray structure analysis.

There have been several attempts to crystallize laccase from different species by various groups without any encouraging results, and these are therefore not documented in the literature. The main reason for this failure is very likely the heterogeneity introduced in the glycosylation of the laccase.

The first crystals of ascorbate oxidase were grown by Ladenstein *et al.* (85) in a final 1.2 M sodium–potassium phosphate buffer, pH 7.0. They were orthorhombic, space group $P2_12_12_1$ with $a = 190.7$ Å, $b = 125.2$ Å, $c = 112.3$ Å, and two molecules (four subunits) per asymmetric unit. Some years later Bolognesi *et al.* (86) obtained a different crystal form of ascorbate oxidase with 2-methyl-2,4-pentane-diol as precipitant. The crystals were orthorhombic as well, space group $P2_12_12$ with $a = 106.7$ Å, $b = 105.1$ Å, $c = 113.5$ Å, and one molecule (two subunits) per asymmetric unit. In both cases, the protein material was prepared from the peels of green zucchini squash (*C. pepo medullosa*). The preliminary three-dimensional X-ray structure of ascorbate oxidase, based on

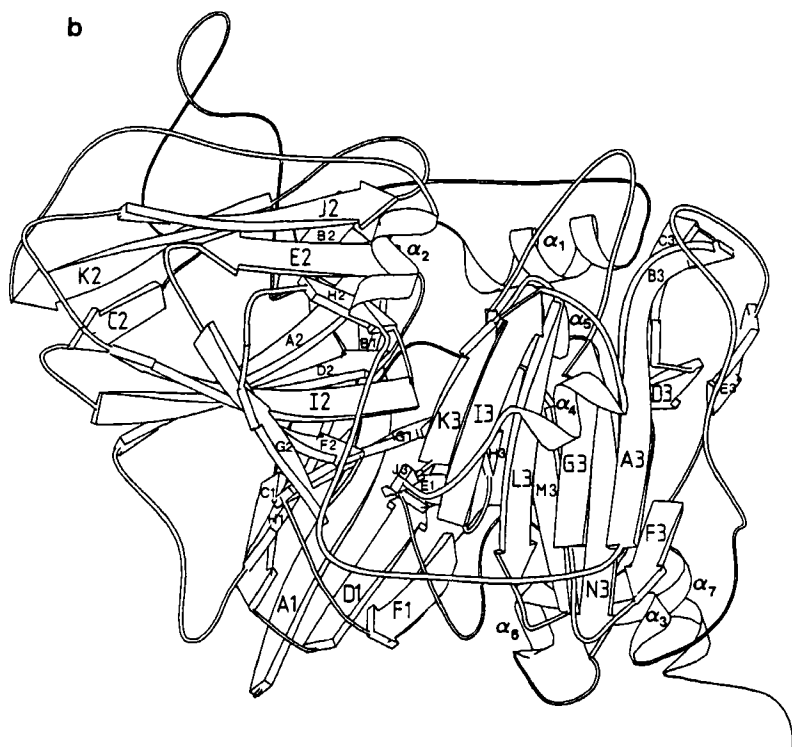
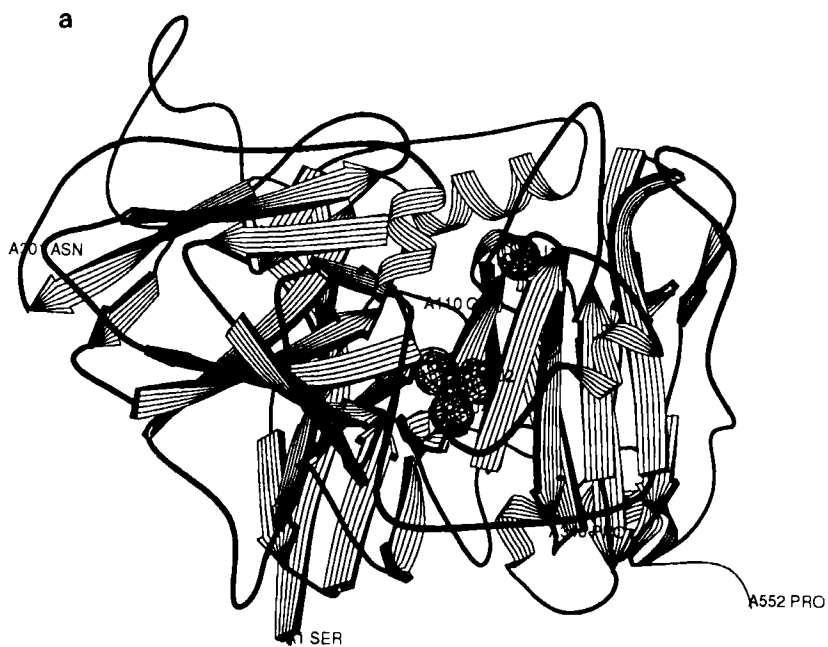
the analysis of both crystal forms, was published in 1989 by Messerschmidt *et al.* (73), and the polypeptide fold and the coordination of the mononuclear blue copper site and unprecedented trinuclear copper site have been described. The structure has now been refined to 1.9 Å resolution and its detailed description has been the subject of another publication (74).

B. OVERALL DESCRIPTION OF THE STRUCTURE

The subunits are arranged in the crystals as homotetramers with D2 symmetry. The structure of a subunit is shown schematically in Fig. 1 (87). Each subunit of 552 amino acid residues has a globular shape with dimensions of $49 \times 53 \times 65$ Å and is built up of three domains arranged sequentially on the polypeptide chain, tightly associated in space. The folding of all three domains is of a similar β -barrel type. It is distantly related to the small blue copper proteins, for example, plastocyanin or azurin. Domain 1 is made up of two four-stranded β -sheets (Fig. 1b), which form a β -sandwich structure. Domain 2 consists of a six-stranded and a five-stranded β -sheet. Finally, domain 3 is built up of two five-stranded β -sheets that form the β -barrel structure and a four-stranded β -sheet that is an extension at the N-terminal part of this domain. A topology diagram of ascorbate oxidase for all three domains and of the related structures of plastocyanin and azurin is shown in Fig. 2. Ascorbate oxidase contains seven helices. Domain 2 has a short α -helix (α_1) between strands A2 and B2. Domain 3 exhibits five short α -helices that are located between strands D3 and E3 (α_3), I3 and J3 (α_4), and M3 and N3 (α_5) as well as at the C terminus (α_6 and α_7). Helix α_2 connects domain 2 and domain 3.

A comparison of the different variants of the β -barrel domain structure in Fig. 1 shows that domain 1 of ascorbate oxidase has the simplest β -barrel with only two four-stranded β -sheets. Plastocyanin and azurin are quite similar but between strands 4 (E1) and 6 (F1) they have insertions of one strand (plastocyanin) or one strand and an α -helix (azurin). Domain 2 has one additional strand H2 in sheet D next to strand E2 (sheet B and strand E1 in domain 1) and two additional strands, F2 and G2, in sheet C next to strand I2 (sheet A and strand F1 in domain 1). Domain 3 resembles domain 2 except for the insertion of the short α -helices and the addition of the four-stranded β -sheet at its N terminus.

The mononuclear copper site is located in domain 3 and the trinuclear copper species is bound between domain 1 and domain 3 (see Fig. 1a). The copper site geometries will be discussed later.



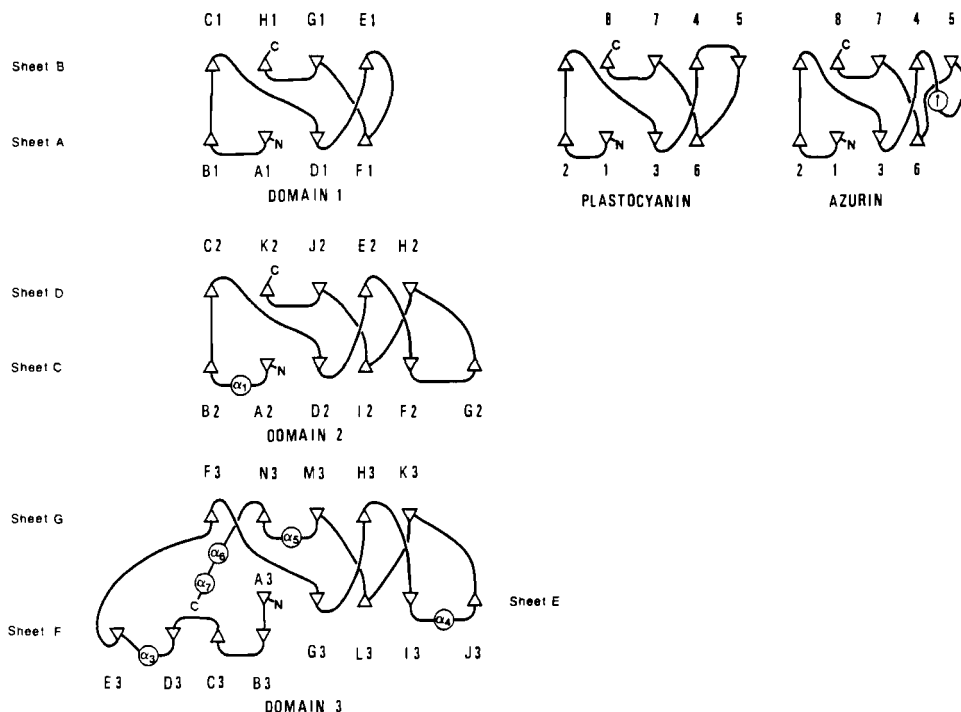


FIG. 2. A topology/packing diagram of the domains of the ascorbate oxidase monomer compared with plastocyanin and azurin. Each β -strand is represented by a triangle whose apex points up or down depending on whether the strand is viewed from the C or N terminus. α -helices are represented by circles.

Each monomer exhibits three disulfide bridges. These are between domain 1 and domain 2 (Cys19–Cys201), between domain 1 and domain 3 (Cys81–Cys538), and within domain 2 (Cys180–Cys193). Three putative attachment sites for *N*-glycosidically-linked carbohydrate moieties are present in the amino-acid sequence of ascorbate oxidase from zucchini (Asn92–Phe93–Thr94, Asn325–Phe326–Thr327, and Asn440–Leu441–Ser442), but only Asn92 shows density for an *N*-acetylglucosamine group.

FIG. 1. A schematic representation of the monomer structure of ascorbate oxidase. (a) Monomer plus copper ions, (b) assignment of the secondary structure elements. β -sheets are represented by arrows, α -helices by helical ribbons. The figure was produced by the RIBBON Program (87).

C. SECONDARY STRUCTURE AND TETRAMER CONTACT SURFACE AREAS

The secondary structure was assigned on the basis of main-chain hydrogen bonding using the algorithm of Kabsch and Sander (88) with a cutoff energy of 0.5 kcal/mol for the definition of a hydrogen bond interaction. Ramachandran plots of the refined models for subunit A and B show that all nonglycine residues lie in or close to energetically allowed regions. All residues with positive Φ -values are located in turns of the polypeptide chain.

There are six α -helices in the monomer of ascorbate oxidase, involving a total of 37 residues or 6.7% of the polypeptide. In addition there are one longer and three short 3_{10} helices. The average conformation angles of these secondary structures for subunit A and B have been calculated and are for both α -helices and 3_{10} helices close to those reported by Barlow and Thornton (89). Exceptions are α_3 and α_5 , which have one $i \rightarrow i + 5$ bond at their C-terminal end to give a short length π -helix.

All turns have been classified according to Crawford *et al.* (90) and Richardson (91). One subunit exhibits 26 reverse turns (10 type 1, 5 type 1', 10 type 2, and 1 type 2'); three reverse, type-1 turns associated with α -helices; three near-reverse turns (one type 1 and two type 2), and three open turns. The preference of glycine at position 3 in the turn is very pronounced. There are three *cis*-proline turns (92) and one Asx turn (93), which displays conventional geometry. The *cis*-prolines have no unusual function in the structure.

The residues involved in the seven β -sheet structures and the hydrogen bonding patterns are shown in Fig. 3. All sheets exhibit the characteristic right-handed twist when viewed along the strand direction. There is a "wide" β -bulge (91) in β -sheet C of domain 2 (Fig. 3b) at residues Val238 and Val239. β -Sheet E of domain 3 (Fig. 3c) contains a classic β -bulge (91) at residues Leu457 and Gly458.

Contact surface areas for the monomer-monomer interactions within the homotetramer present in both crystal forms were calculated using the algorithm of Lee and Richards (94). It is evident from these calculations (74) that the contact surface areas between the two dimers about the crystallographic dyad are by far the largest. Ascorbate oxidase

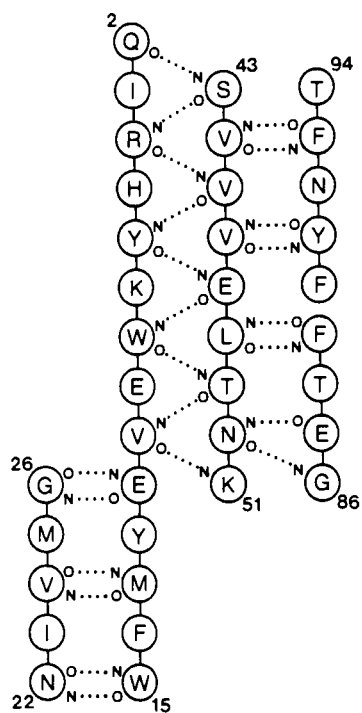
FIG. 3. Main-chain hydrogen bonding scheme of the seven β -sheets in ascorbate oxidase. (a) Domain 1. (b) Domain 2; wide β -bulge: $x \rightarrow 264$, $1 \rightarrow 238$, $2 \rightarrow 239$. (c) Domain 3; classic β -bulge: $x \rightarrow 492$, $1 \rightarrow 457$, $2 \rightarrow 458$. The amino acid residues are indicated by the one-letter code.

a

DOMAIN 1

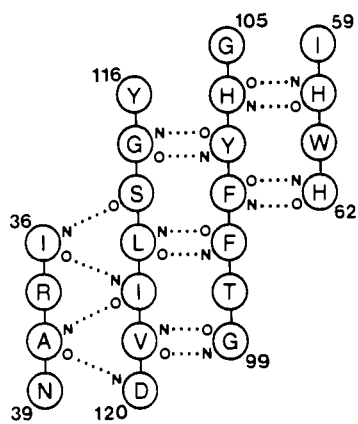
Sheet A

B1 A1 D1 F1



Sheet B

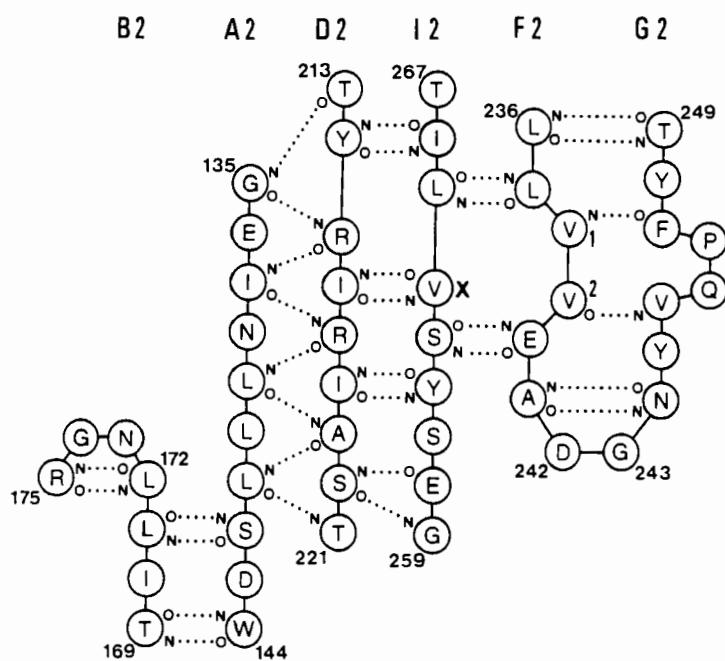
C1 H1 G1 E1



b

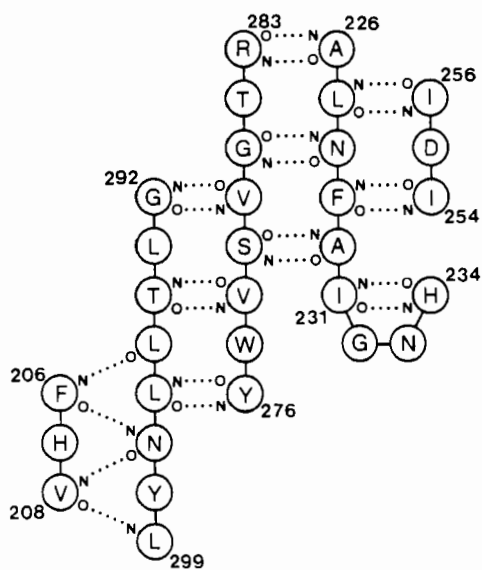
DOMAIN 2

Sheet C

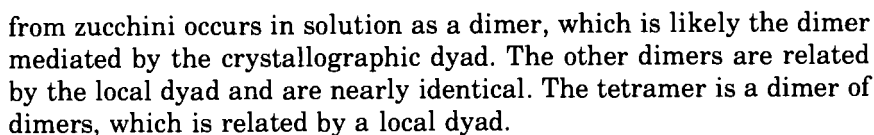


Sheet D

C2 K2 J2 E2 H2



DOMAIN 3



D. COPPER SITE GEOMETRIES

The mononuclear copper site is located in domain 3 and has the four canonical type-1 copper ligands (His, Cys, His, and Met) also found in plastocyanin and azurin. It is coordinated to the ND1 atoms of His 445 and 512, the SG atom of the Cys 507, and the SD atom of Met 517 in a distorted trigonal pyramidal geometry. The SD atom is at the long apex (see Fig. 4). Bond lengths of the type-1 copper for both subunits are displayed in Table III. They are compared with oxidized poplar plastocyanin (95) and azurin from *Pseudomonas aeruginosa* (96). Figure 5 shows an overlay of the type-1 copper site in azurin, plastocyanin, and ascorbate oxidase.

The copper is penta coordinated in azurin (glycine) with the main-chain carbonyl oxygen of the residue preceding the first histidine copper ligand on the polypeptide chain. This carbonyl oxygen forms the fifth ligand. In poplar plastocyanin, the homologous peptide is a proline at the beginning of a turn, causing the carbonyl oxygen to be removed to a distance of 3.8 Å from the type-1 copper ion. In ascorbate oxidase, the corresponding strand is extended, moving the carbonyl oxygen to a distance of 4.8 Å from the type-1 copper ion. This extended strand contributes Glu443 to the formation of the binding site of the reducing substrate (74).

The trinuclear copper site (see Fig. 6) has eight histidine ligands symmetrically supplied by domain 1 and domain 3 and two oxygen ligands. Seven histidines are ligated by their NE2 atoms to the copper ions, whereas His62 is ligated to CU3 K3 by its ND1 atom. In the

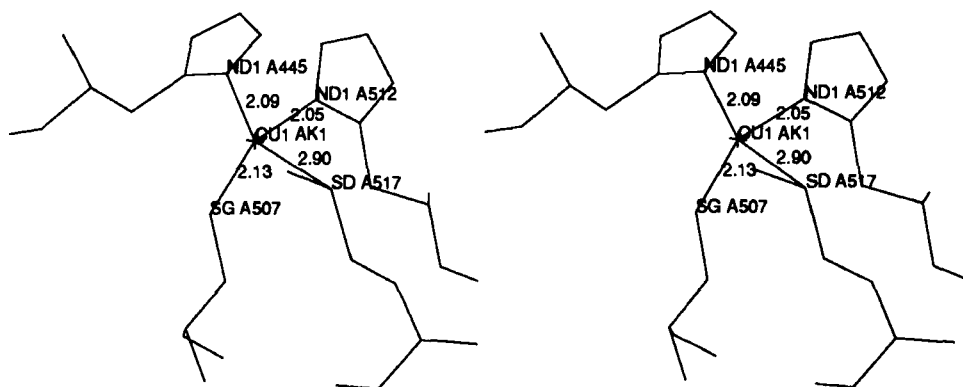


FIG. 4. Stereo drawing of the type-1 copper site in domain 3. The displayed bond distances are for subunit A.

TABLE III

COPPER–COPPER AND COPPER–LIGAND DISTANCES IN ASCORBATE OXIDASE
COMPARED WITH COPPER–LIGAND DISTANCES FOR THE TYPE-1 COPPER SITE IN
PLASTOCYANIN AND AZURIN

Atom 1	Atom 2	Distance (Å)		Azurin ^a		Plastocyanin ^b
		A	B	wtp5	wtp9	
CU1 K1	CU2 K3	12.20	12.20			
CU1 K1	CU3 K3	12.73	12.65			
CU1 K1	CU4 K3	14.87	14.86			
Type-1 copper site						
CU1 K1	ND1 445 ^c	2.10	2.12	2.11	2.09	2.04
CU1 K1	SG 507	2.13	2.03	2.25	2.26	2.13
CU1 K1	ND1 512	2.05	2.11	2.03	2.04	2.10
CU1 K1	SD 517	2.90	2.83	3.15	3.12	2.90
CU1 K1	O 444	4.78	4.83	2.97	2.95	3.82
Trinuclear copper site						
CU2 K3	CU3 K3	3.68	3.73			
CU2 K3	CU4 K3	3.78	3.90			
CU3 K3	CU4 K3	3.66	3.69			
CU2 K3	NE2 106	2.16	2.17			
CU2 K3	NE2 450	2.06	2.09			
CU2 K3	NE2 506	2.07	2.09			
CU3 K3	ND1 62	1.98	2.13			
CU3 K3	NE2 104	2.19	2.14			
CU3 K3	NE2 508	2.14	2.08			
CU4 K3	NE2 60	2.00	2.02			
CU4 K3	NE2 448	2.09	2.05			
CU2 K3	OH1 K3	2.00	2.00			
CU3 K3	OH1 K3	2.06	2.00			
CU4 K3	OH3 K3	2.02	2.03			

^a The wtp5 and wtp9 recombinant wild-type structures are from *Pseudomonas aeruginosa* azurin at pH 5.5 and 9.0. The data are from Nar *et al.* (96).

^b Plastocyanin is from poplar leaves. The data are from Guss and Freeman (95).

^c Ascorbate oxidase numbering.

preliminary structural report on ascorbate oxidase (73) based on lower resolution data, all eight histidine residues were modeled with their NE2 atoms as ligands to the copper atoms of the trinuclear site. The high-resolution data allow an unequivocal interpretation. His62 is part of a β -sheet, whereas His450 is not. An overlay of the relevant parts of domain 3 onto domain 1 show that His62 comes closer with its main-

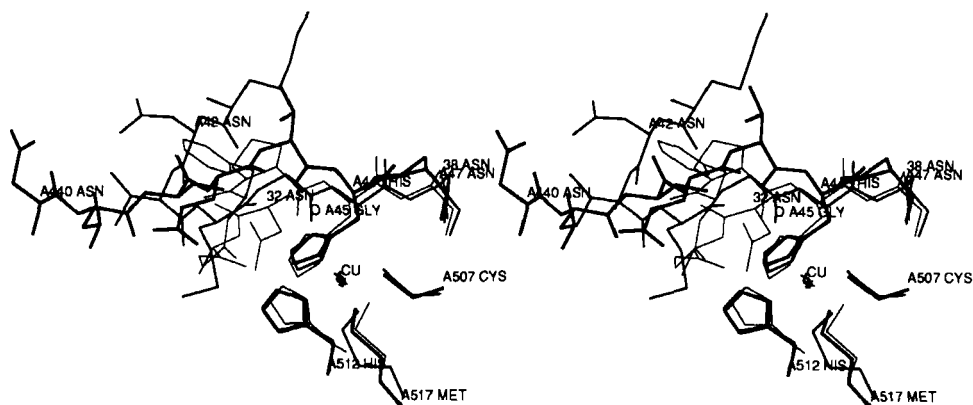


FIG. 5. Stereo plot of the overlay of the type-1 copper sites for poplar plastocyanin (thin line), *Pseudomonas aeruginosa* azurin (medium line), and ascorbate oxidase (thick line).

chain atoms to the copper ion CU3 than the corresponding atoms of His450. As a consequence, the side chain of His62 has to adopt a conformation in which ND1 of the imidazole ring is ligated to the copper ion CU3.

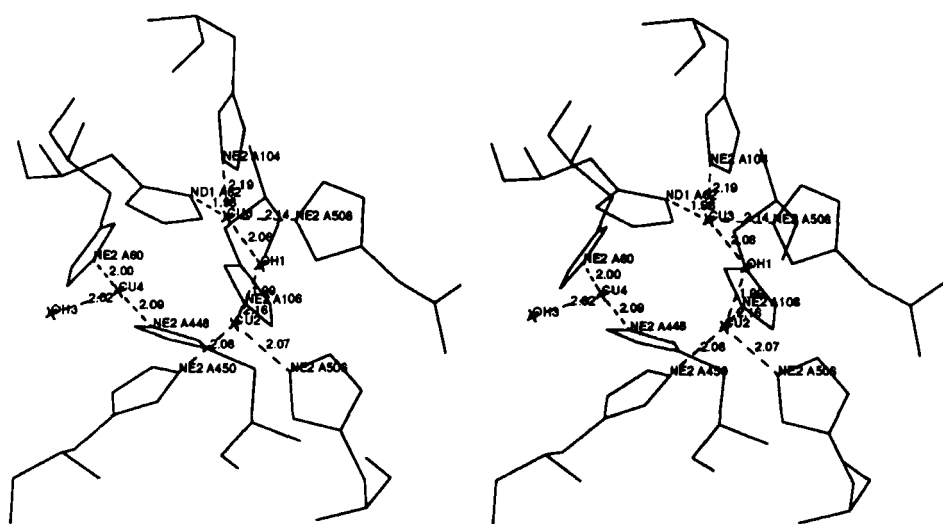


FIG. 6. Stereo drawing of the trinuclear copper site. The displayed bond distances are for subunit A.

The trinuclear copper site may be subdivided into a pair of coppers (CU2 K3 and CU3 K3) with six histidine ligands in a trigonal prismatic arrangement. The pair is bridged by an OH^- or O^{2-} , which leads to a strong antiferromagnetic coupling and makes this copper pair EPR silent. The pair very likely represents the spectroscopic type-3 copper. The remaining copper (CU4 K3) has two histidine ligands and an OH^- or H_2O ligand and probably represents the spectroscopic type-2 copper. Both oxygen ligands could be clearly detected from difference Fourier maps. An oxygen ligand in the center of the three copper ions could not be detected.

Cole *et al.* (97) studied the electronic structure of the laccase trinuclear copper active site by the use of absorption, circular dichroism, and low-temperature magnetic circular dichroism spectroscopies. The assigned ligand field transition energies indicated that all three coppers have tetragonal geometries and that the two type-3 coppers are inequivalent.

The latter interpretation fits well with our structural model as CU3 K3 of the copper pair is ligated to one ND1 and two NE2 atoms, but the former interpretation, tetragonal coordination geometries for all three coppers, is not consistent with the structure. The coppers of the pair are both tetrahedrally coordinated, whereas the type-2 copper has three ligands. The existence of a central oxygen ligand would give rise to a penta coordination of both copper pair atoms (but not a tetragonal-pyramidal coordination) and a square-planar coordination for the spectroscopic type-2 copper. Messerschmidt *et al.* (74) examined by modeling whether, by side chain torsion angle rotations, His62 and His450 could become bridging ligands between CU4 K3 and CU2 K3 or CU3 K3 with both ring nitrogens as ligating atoms but found this stereochemically unreasonable.

The copper-copper and copper-ligand distances of the trinuclear copper site are displayed in Table III for both subunits. Their mean values ($\text{Cu}-\text{N}$, 2.09 Å ($\sigma = 0.06$ Å); $\text{Cu}-\text{O}$, 2.02 Å ($\sigma = 0.02$ Å)) are comparable to those of binuclear copper model compounds with nitrogen and oxygen copper ligands (98, 99) in the range of 0.1 Å for the copper ligand bonds. There is no long $\text{Cu}-\text{N}$ bond (about 2.7 Å) as found in the binuclear copper center of hemocyanin from *Panulirus interruptus*, determined by X-ray crystallography at 3.2 Å resolution (100). The binuclear copper center in hemocyanin has a trigonal antiprismatic arrangement of the six histidine ligands, whereas the type-3 coppers in ascorbate oxidase show the trigonal prismatic coordination. The presence of the type-2 copper and its ligands would not allow the former arrangement.

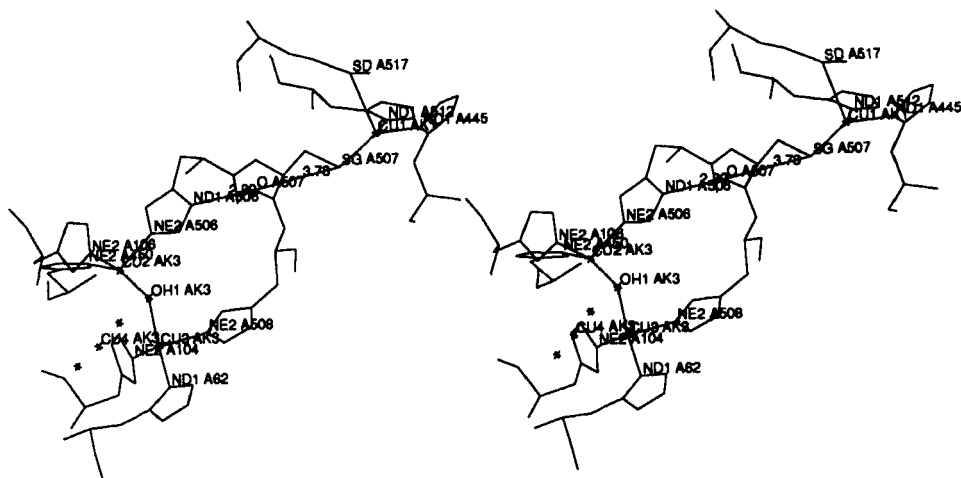


FIG. 7. Stereo drawing of the region of the atomic model containing the type-1 copper center in domain 3 and the trinuclear copper center between domain 1 and domain 3.

The average copper–copper distance in the trinuclear copper site of ascorbate oxidase is 3.74 Å ($\sigma = 0.08$ Å) and the individual distances do not deviate by more than 0.16 Å from this mean value. The average copper–copper distance in hemocyanin is 3.54 Å (100). The copper–copper distances are too long for copper–copper bonds but magnetic interactions are possible.

The shortest distance between the type-1 copper center and the trinuclear copper center is 12.2 Å. The His506–Cys507–His508 amino-acid sequence segment links the type-1 copper center and the type-3 copper center as a bridging ligand (see Fig. 7). Aspects of the intramolecular electron transfer between the two redox centers will be discussed in Section XII.

V. Structural Relationships among the Blue Copper Oxidases

A. AMINO-ACID SEQUENCE ALIGNMENT

Knowledge of the three-dimensional structure of ascorbate oxidase and of amino-acid sequences of all members of the blue oxidases made it possible to carry out a structurally based amino-acid sequence alignment (101) involving *N. crassa* laccase, cucumber ascorbate oxidase, and human ceruloplasmin. The structural basis of this alignment was

the spatial superposition of the three domains of ascorbate oxidase, which allowed recognition of the conserved and variable structural elements within the single domains.

The amino-acid sequence similarity of the blue oxidases supports a domain structure of ceruloplasmin and laccase. Ceruloplasmin has six and laccase, three domains, which are related to the domains of ascorbate oxidase. These domains have variable lengths over 125–200 residues but show a common β -barrel motif in which β -strands and turns may be superimposed in all domains. The occurrence of β -barrel motifs in laccase and ceruloplasmin are solely based on sequence homology with ascorbate oxidase. The variable parts of the ascorbate oxidase domains are mainly in connecting segments and correspond to the regions of weak similarity in the aligned sequences. Similarity is high in segments of the conserved secondary structure. These conserved elements include the copper ligands.

Comparison of the amino-acid sequences of laccase and ascorbate oxidase shows that they are more closely related among each other than to ceruloplasmin. Fungal *N. crassa* laccase contains all the copper ligands of ascorbate oxidase, except methionine of type-1 copper. It forms a disulfide bridge (116–537) between domain 1 and domain 3 as ascorbate oxidase (disulfide bridge 83–541). The spatial structure of laccase is expected to be very similar to that of ascorbate oxidase, including the type-1 copper in domain 3 and the trinuclear copper site with its ligands between domain 1 and domain 3. Ascorbate oxidase is a symmetrical dimer of two laccase-like subunits. Dimerization is promoted by a metal ion, whose nature is not yet established. This metal is located on the molecular dyad and has two histidine ligands (His 286) supplied symmetrically from each subunit (73). The existence of six structurally related domains in ceruloplasmin is supported by the known disulfide bridges. SS bridges 155–188, 515–541, and 855–881 are similar to 100–124, 273–302, and 503–527 in ascorbate oxidase according to the amino-acid sequence alignment (101). The corresponding positions in ascorbate oxidase in domains 1, 2, and 3 are at distances of about 5.0 Å so that disulfide bridges may be formed. A similar disulfide bridge (300–334) can be formed in domain 2 of *N. crassa* laccase (101).

Two other SS bridges in ceruloplasmin, 257–338 and 618–699, are similar to 41–124 and 424–525 of ascorbate oxidase. Also these disulfide bridges can be formed easily.

The tryptic cleavage sites for ceruloplasmin are at the end of the domains but approximately follow the internal triplication. A fourth cleavage site is in the middle of domain 3 in an extended and variable

region of the secondary structure. The tryptic cleavage sites are in accord with the six-domain structure.

Human ceruloplasmin shows sequence similarities to the human blood clotting factors VIII (102) and V (103). The amino-acid sequence of human factor VIII consists of 2332 residues. It exhibits three distinct types of structural domains, including a triplicated region of ~330 amino acids (A domain), a unique region of 980 amino acids (the B domain), and a C-terminal duplicated region of 150 amino acids (C domain), which are arranged in the order A1–A2–B–A3–C1–C2. The A domains of factor VIII show significant similarity to ceruloplasmin. The A domains can each be subdivided into two domains and may form disulfide bridges as in ceruloplasmin because the corresponding cysteines are present. A1 and A3 contain the canonical ligands for a type-1 copper at the homologous positions in the amino-acid sequence. The four His–X–His sequences, ligands to the trinuclear copper site, are not found in factor VIII, however.

About 40% (938 residues) of the amino-acid sequence of factor V has been established (103). It shows similarities to the amino-acid sequences of human ceruloplasmin and human factor VIII. The partial sequence contains a region that is similar to domains 5 and 6 in ceruloplasmin and A3 in factor VIII. However, it does not have the canonical ligands for type-1 copper or the trinuclear copper site. On the other hand, cysteine residues are present at the homologous position of ceruloplasmin. They form a disulfide bridge in this structure.

B. STRUCTURAL MODEL OF THE COPPER SITES FOR CERULOPLASMIN

Ceruloplasmin also contains the trinuclear copper site established for ascorbate oxidase. The four His–X–His sequences, providing the ligands for this copper site, are divided equally between domains 1 and 6 of ceruloplasmin (101). Ligands for type-1 copper in suitable spacings on the polypeptide chain are in domains 2, 4, and 6, assuming the nearly isosteric methionine and leucine as equivalent. *Neurospora crassa* laccase apparently forms a blue copper site with His, Cys, His, and Leu at the canonical positions for the ligands of the type-1 copper site. The copper has three protein ligands, two His and one Cys, at this site, because the leucine, isosteric to methionine, cannot be considered a copper ligand. It has a very high redox potential of 780 mV. Recently, it has been shown, using a recombinant Met–121–Leu mutant of azurin from *P. aeruginosa*, that the methionine of the type-1 copper site is not required to generate the properties of this metal site (104). The putative

type-1 copper site in domain 2 of ceruloplasmin also has a leucine and is expected to have a high redox potential.

Redox titrations of ceruloplasmin, indeed, show two different standard redox potentials with values of 490 and 580 mV (105). The reoxidation of the completely reduced enzyme by dioxygen as measured at 630 nm proceeds in two steps. About half of the blue color returns fast (within milliseconds), whereas the complete reaction requires several hours. Therefore, it was proposed (106) that only one of the type-1 coppers is involved in the four-electron transfer to oxygen and thus forms a part of the active site. This copper has been called the "fast" type 1. The type-1 copper in domain 6, which may interact with the trinuclear copper, has been interpreted to be a fast species, explaining most of the fast reoxidation amplitude. The slight quantitative discrepancy may be due to experimental errors (101). The assignment of the three type-1 copper centers was proposed by Ortel *et al.* (107) and later by Moshkov *et al.* (108), but the assignment of the ligands for the type-2 and type-3 coppers by Rydén (109) and later Moshkov *et al.* (108) is incompatible with the 3D structure of the related blue oxidase ascorbate oxidase.

The six-domain structure and copper site model for ceruloplasmin received further support from the elucidation of the X-ray structure of a copper-containing nitrite reductase from *Achromobacter cycloclastes* (110). This nitrite reductase occurs in solution and in the crystal as a homotrimer. The trimer shows C3 symmetry. One monomer is built up of two domains of a similar β -barrel fold as found in the small blue copper proteins or in ascorbate oxidase (see Fig. 8a). The enzyme contains two mononuclear copper centers. A type-1 copper site with the canonical ligands (His, Cys, His, and Met) is located in domain 1 and a type-2 copper with three histidines and one water molecule as ligands is bound between domain 1 and domain 2 of the adjacent symmetry-related molecule (see Figs. 8a and 8b). The copper-containing domains of ascorbate oxidase can be superimposed on the domains of nitrite reductase, which are displayed in Fig. 8b. The type-1 copper and its ligands in nitrite reductase fall at the type-1 center of ascorbate oxidase, and all three histidines of the type-2 site, as well as the copper, fall at the same site as the trinuclear cluster of ascorbate oxidase (110) (Figs. 8b and 8c). Sequence comparison (111) shows that two histidines from domain 1 (residues 100 and 135) and two from domain 2 (residues 255 and 306) correspond to four of the eight histidine ligands of the trinuclear copper cluster in ascorbate oxidase. In nitrite reductase only histidine residues 100, 135, and 306 are ligands. These comparisons

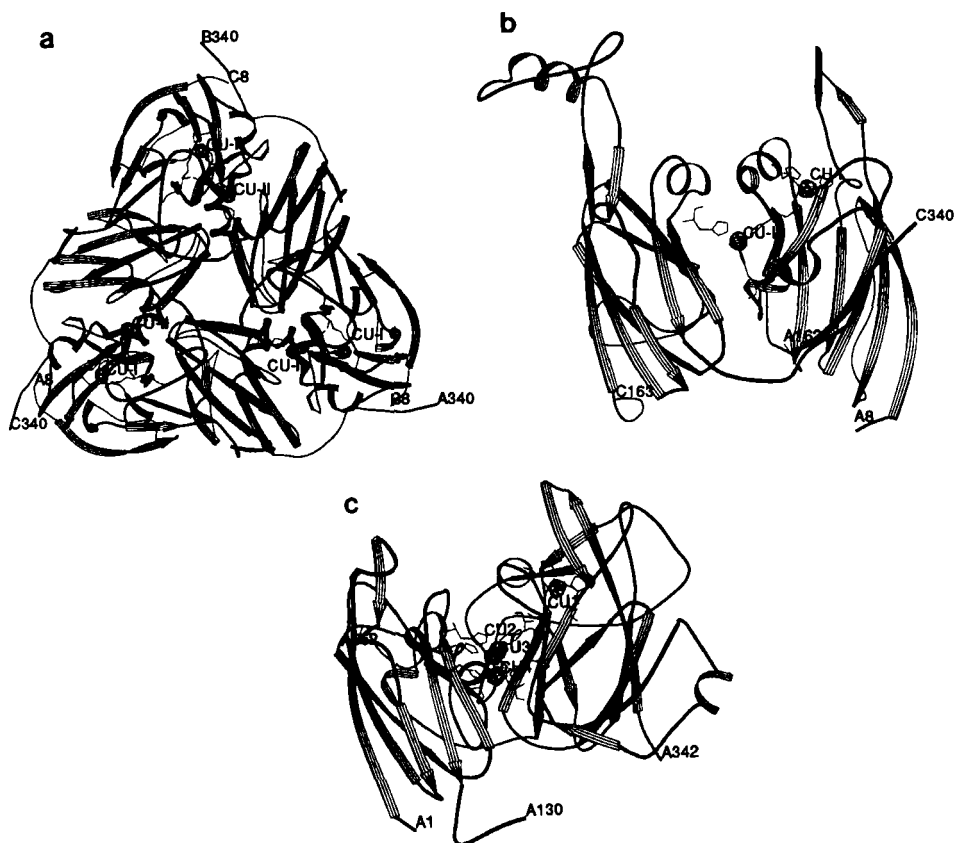


FIG. 8. (a) Drawing of the trimer of nitrite reductase from *Achromobacter cycloclastes*. (b) Drawing of the interface between domain 1 (subunit A) and domain 2 of the adjacent symmetry-related molecule (subunit C) of nitrite reductase from *A. cycloclastes*. (c) Drawing of domain 1 and 3 of ascorbate oxidase. The type-1 copper is in domain 3 and the trinuclear copper center is between domain 1 and domain 3. The domains have an orientation similar to that of the corresponding domains of the nitrite reductase shown in b. The figure was produced by the RIBBON Program (87).

suggest that the type-2 copper of nitrite reductase corresponds to one of the type-3 copper pair in ascorbate oxidase.

In the trimer of nitrite reductase a six-domain structure is realized, which is reminiscent of the six-domain structure of ceruloplasmin (112), which was deduced from the amino-acid sequence alignment with the other blue oxidases (101). However, the arrangement of the six gene segments in ceruloplasmin is not simply a triplication of an ancestral

nitrite reductase gene coding for two domains, but the triplication of a gene in which the segments coding for the individual domains were inverted. This is due to the finding that the type-1 copper sites in ceruloplasmin are found in domains 2, 4, and 6 rather than in domain 1 and symmetrical counterparts in nitrite reductase.

VI. Fungal Laccases, Ascorbate Oxidases, and Related Proteins

There are now five known amino-acid sequences of fungal laccases and three of ascorbate oxidases, as mentioned earlier. Furthermore, amino-acid sequences of three different proteins that are related to the blue oxidases have been reported. The first of them is phenoxazinone synthase from *Streptomyces lividans* (113). This enzyme is a copper-containing oxidase that catalyzes the coupling of 2-aminophenols to form the 2-aminophenoxazinone chromophore (114). This reaction constitutes the final step in the biosynthesis of the potent antineoplastic agent actinomycin. The second one is the gene product of a copper resistance gene of *Pseudomonas syringae* pv. *tomato* (115). This protein is believed to function as a copper-binding protein, thus making a contribution to the copper resistance. The third one is a product of the Bp10 gene of *Brassica napus* (rape) (116). The expression of the Bp10 gene family is pollen specific and developmentally regulated.

A multiple amino-acid sequence alignment of these 11 related proteins has been carried out and is shown in Table IV. The basis of this alignment was the three-dimensional structure of ascorbate oxidase. Ceruloplasmin has been omitted because it consists of a triplication of a two-domain structure and not of a three-domain structure as is valid for all the proteins included in this alignment. All protein copper ligands characteristic of the blue oxidases are conserved with two principal exceptions. The rape Bp10 gene product has only one histidine of the copper ligands conserved, meaning that this protein will bind no copper and therefore will have no oxidase activity (116). The second exception concerns the position for a possible fourth ligand of the type-1 copper. As mentioned above, there is very often a methionine at this place in small blue copper proteins as well as in blue oxidases. This methionine serves as a weak ligand to the type-1 copper. In *A. nidulans* laccase, the three ascorbate oxidases, phenoxazinone synthase, and the copper-binding protein from the *P. syringae* copper resistance gene, there is a methionine at this position. Similar to *N. crassa* laccase, *P. radiata* and *C. parasitica* laccase also contain a leucine at this place. The explanations of *N. crassa* laccase related to the spectral and electro-

TABLE IV

STRUCTURALLY BASED AMINO-ACID SEQUENCE ALIGNMENT OF FUNGAL LACCASES, ASCORBATE OXIDASES, AND RELATED PROTEINS^a[illegible]

[illegible]

(continues)

A.n. 305 S N L A P L T N A A A P G L P E - - - - V G G V D L A L N F N L T F D G P S L K F Q I N G V - T F V 349
P.r. 303 V D L H P L A T M A V P G S P V - - - - A G G V D T A I N F N L T F D G - - T N F F I N G A - S F V 345
C.h. 355 - - - - - - - - - - - - - - - - L N T G N T I P I T - - L D G F - V W R V N G T A - - - 376
N.c. 390 - - - - - - - - - - - - - - - - D N T L D V Q L S T - - T T R - - K W T I N G S - T L D 412
Cr.p. 331 R I F A A M G S P K P P V R Y - - - - - N R R L F L L N T Q N R I N G F M K K W A I N N V S L A L 373
AO c. 329 R I T A A M G S P K P P V K S - - - - - N R R I F L L N T Q N V I N G Y V K K W A I N D V S L A L 371
AO z. 329 R I T A A M G S P K P P V K F - - - - - N R R I F L L N T Q N V I N G Y V K K W A I N D V S L A L 371
PS 331 R R L R L V D K G P G 341
COPA
BP 308 N L T A S A A R P N P Q G S Y H Y G K I N I T R T I K L V N T Q G K V D G K L R F A L N G V S L A L 357

L I N
| β β A3 β β | | β B3 β | | β C3 β | | β D3 β |

A.n. 350 P P T V P V - - - - - - - - - - L L Q I L S G A Q S A - - - - - A D L L P S G S V 375
P.r. 346 P P T V P V - - - - - - - - - - L L Q I I S G A Q N A - - - - - Q D L L P S G S V 371
C.h. 377 - - - - - I N I N W N K P V L E Y V M T G M T N Y - - - - - S Q S D N I V Q 404
N.c. 413 - - - - - V D W G H P I T Q Y V I N K S T A W - - - - - P S T D N V W L 438
Cr.p. 374 P P T P Y L A A M K M R L N T A F N Q N P P P E T F P L N N Y D I N N P P P N P E T T T G N G V Y K F 423
AO c. 372 P P T P Y L G A M K F N L L H A F D Q N P P P E V F P E D Y D I D T P P T N E K T K I G N G V Y Q F 421
AO p. 372 P P T P Y L G A M K Y N L L H A F D Q N P P P E V F P E D Y D I D T P P T N E K T R I G N G V Y Q F 421
AO z. 451 F N D G L F 457
PS 518 A D A Q P L I 524
COPA
BP 358 P P T P - - - - - L K L A E Y F G I S D K V F K Y D T I T D D P T P E Q I K N I K I E P N V L N I 401

P P T

| α α₃ α |

| β E3 β | | β F3 β |

A.n. 503 L I H - P P H P I H K H G N R A Y I I G N G V G K F R W E N 531
P.c. 376 - Y A L P S N A T I E L S L P A G - - A L G - G P H P P H L H G H T F S V V R P A G S T T Y N Y V - 420
C.h. 372 - Y S L P S N A D I E I S F P A T A A A P G - A P H P P H L H G H A F A V V R S A G S T V Y N Y D - 418
N.c. 405 - V E G V N Q W K Y W L I E N D P D G A F S - L P H P I H L H G H D F L I L G R S P D V T A I S N T 452
Cr.p. 439 - V E E A N Q W A Y W L I E N D P T A T G N A L P H P I H L H G H D F V V L G R S P N V S P T A - - 485
AO c. 424 - N M G E T V D V I L Q N A N M L N P N M S - E I H P W H L H G H D F W V L G Y G E G K F Y A P E D 471
AO p. 422 - K I G E I V D V I L Q N A N M M K E N L S - E I H P W H L H G H D F W V L G Y G D G K F - T A E E 468
AO c. 422 - K I G E V V D V I L Q N A N M M K E N L S - E I H P W H L H G H D F W V L G Y G D G K F - S A E E 468
PS 458 - T I G E G T H E Q W T F L - - - - - N L S P I L H P M H I H L A D F Q V L G R D A 493
COPA 525 L K Y G E R V R I V L V N D T - - - - - M M T H P I H L H G M W S D L E D 556
BP 402 - T H R T F V E V F E N H E - - - - - K - S V Q S W H L D G Y S F F S V A V E P G T W - T P E K 442

G

| β β G3 β β |

*1 *2 *3
H P H L H G H D F V L G
| β H3 β | | β β β I3 β β |

P.c. 495 T H L I T S G F A S I I Q W M M G G N G L F A P H A L S F L G S Q • 527
 C.h. 496 V N D Q • 499
 N.c. 445 P D N A P F P K D D S G L R S G V K A R E V K M K W • 570
 Cr.p. 579 P S K D I F K Q D D S G V • 591
 AO c. 549 N Y P R L P • 554
 AO p. 546 I N N P • 549
 AO z. 546 I N N P K N P • 552
 PS
 BP 522 N T P K • 525

Note. A.n., laccase from *Aspergillus nidulans* (40); P.r., laccase from *Phlebia radiata* (32); C.h., laccase from *Coriolus hirsutus* (41); N.c., laccase from *Neurospora crassa* (39); Cr.p., laccase gene from *Cryphonectria parasitica* (37); AO c., ascorbate oxidase from cucumber (51); AO p., ascorbate oxidase from pumpkin (52); AO z., ascorbate oxidase from zucchini (53); PS, phenoxazinone synthase from *Streptomyces lividans* (113); COPA, copper binding protein from the copper resistance gene from *Pseudomonas syringae* pv. *tomato* (115); BP, *Brassica napus* Bp10 gene product (116). Alignment positions with greater than or equal to six identities are indicated. The secondary structure elements, known from the three-dimensional structure of ascorbate oxidase, are given at the bottom of each alignment block. *1, ligand to type-1 copper; *2, ligand to type-2 copper; *3, ligand to type-3 copper. Parts of sequences were omitted from the alignment when no relationship could be detected.

^o Ceruloplasm is omitted.

chemical properties of such a type-1 site should be valid as well. *Coriobacterium hirsutus* laccase holds a phenylalanine at this position. This residue also cannot serve as a copper ligand. The role of the residue located in this position seems to be to tune the redox potential of the type-1 copper site, which is necessary for the function of the enzyme.

An inspection of this amino-acid sequence alignment shows that the sequences align very well in the segments of the conserved copper ligands and quite well in segments of the defined secondary structure elements of the ascorbate oxidase structure. The alignment is unacceptable for *A. nidulans* laccase between domains 2 and 3 and for phenoxazinone synthase and the bacterial copper-binding protein in domain 2 and at the beginning of domain 3. On the other hand, the rape Bp10 gene product aligns very well on ascorbate oxidase (see also Table V).

TABLE V

SIMILARITY MATRIX FOR THE AMINO-ACID SEQUENCE ALIGNMENT DISPLAYED IN TABLE IV^a

Source ^b	Number of differences										
	1	2	3	4	5	6	7	8	9	10	11
a. The complete amino acid sequence alignment displayed in Table IV, included in calculations											
A.n.	0.00	503.00	477.00	501.00	522.00	518.00	518.00	521.00	393.00	374.00	528.00
P.r	87.02	0.00	195.00	535.00	568.00	463.00	463.00	465.00	484.00	483.00	500.00
C.h.	86.26	36.52	0.00	524.00	551.00	437.00	438.00	443.00	462.00	452.00	484.00
N.c.	85.93	84.38	83.31	0.00	309.00	540.00	541.00	543.00	537.00	525.00	581.00
Cr.p.	86.86	85.54	85.56	50.49	0.00	553.00	558.00	561.00	557.00	545.00	593.00
AO c.	87.80	77.68	76.40	84.24	83.53	0.00	109.00	108.00	495.00	499.00	407.00
AO p.	88.10	77.95	77.11	84.40	84.29	19.68	0.00	16.00	488.00	492.00	411.00
AO z.	88.16	78.28	77.58	84.71	84.74	19.46	2.90	0.00	490.00	496.00	415.00
PS	90.97	90.98	91.49	92.75	92.99	88.24	87.77	87.66	0.00	176.00	502.00
COPA	89.47	91.13	89.86	91.46	91.91	89.43	88.97	89.21	80.73	0.00	489.00
BP	91.35	84.75	85.82	89.66	88.91	71.28	72.36	72.68	93.83	92.26	0.00
b. Segments 1–63, 205–547, 579–608, and 653–712 from the amino acid sequence alignment displayed in Table IV, omitted from calculations											
A.n.	0.00	145.00	144.00	134.00	138.00	136.00	138.00	138.00	172.00	156.00	163.00
P.r.	71.08	0.00	50.00	138.00	137.00	132.00	128.00	130.00	166.00	156.00	165.00
C.h.	70.24	24.75	0.00	132.00	136.00	128.00	127.00	129.00	169.00	153.00	168.00
N.c.	67.00	66.99	64.08	0.00	66.00	129.00	130.00	132.00	169.00	153.00	159.00
Cr.p.	68.66	66.18	65.70	33.00	0.00	125.00	126.00	128.00	169.00	152.00	157.00
AO c.	68.34	64.71	62.75	64.82	62.19	0.00	26.00	26.00	154.00	146.00	134.00
AO p.	69.35	63.37	62.87	65.33	62.69	13.20	0.00	4.00	151.00	142.00	136.00
AO z.	69.35	64.36	63.86	66.33	63.68	13.20	2.06	0.00	150.00	143.00	137.00
PS	83.90	80.58	81.64	82.44	82.44	75.49	75.12	74.63	0.00	130.00	182.00
COPA	78.00	76.85	75.00	76.12	76.00	73.00	72.08	72.59	76.47	0.00	162.00
BP	80.69	79.71	80.77	78.33	76.59	66.67	68.00	68.50	88.78	81.41	0.00

^a Results are given as percent difference.^b See Table IV for definition.

VII. Evolution of the Blue Oxidases and Related Proteins from a Common Ancestor

Dwulet and Putnam (117) proposed that ceruloplasmin had evolved from a fused azurin gene and, more recently, Rydén (118) speculated about an evolution of the blue oxidases from a common ancestor, suggesting that an ancestral gene was first duplicated. The simple oxidases like laccase or ascorbate oxidase then acquired a third genetic element, whereas a triplication of the duplicated gene lead to ceruloplasmin. This evolution scheme can be checked by calculation of a similarity matrix based on the amino-acid sequence alignment given in Messerschmidt and Huber (101) and in Table IV. The program ALNED (119) was used to calculate the similarity matrices. Table V displays similarity matrices computed for the amino-acid sequence alignment shown in Table IV. The calculations for Table Va included all residues, whereas in Table Vb the alignment segments 1–63, 205–547, 579–608, and 653–712 are omitted (numbering of alignment starts at residue 1 of *C. parasitica* laccase).

The similarity matrix calculated in Messerschmidt and Huber (101) indicates clearly the six-domain structure of ceruloplasmin and three-domain structures for laccase and ascorbate oxidase. The internal triplication within the ceruloplasmin amino-acid sequence is reflected by values of about 60% difference. Comparison of both the N-terminal domains and the C-terminal domains of the blue oxidases indicates, respectively, a relationship that is closer and relevant values for percent difference that are significantly lower than those for other comparisons. This might reflect the requirements for the trinuclear copper site. The lowest values of about 70 to 73% difference are observed for both N-terminal and C-terminal domains of laccase and ascorbate oxidase, showing that the two oxidases are more closely related to ceruloplasmin than either of them.

Table V supplies insight into the relatedness within fungal laccases and ascorbate oxidases and to the other included proteins. Obviously both Tables Va and Vb show the same trend. The laccases of the narrowly related basidiomycetes *P. radiata* and *C. hirsutus* show differences of only 37%. The differences for the laccases from the ascomycetes *N. crassa* and *C. parasitica* are about 50%. The laccase of the deuteromycete *A. nidulans* shows very low identities to all partners of the alignment when all residues are included into the calculations (Table Va). The picture becomes clearer when badly aligning segments are omitted from the calculations (Table Vb). The differences from the other lac-

cases and the ascorbate oxidase are about 70% and from the other three proteins about 80%. It is interesting to note that it appears from this study that *A. nidulans* and the ascomycete laccases are equally related to the other fungal laccases and the plant enzyme ascorbate oxidase. The basidiomycete laccases appear to be even more closely related to ascorbate oxidase than to the other fungal laccases.

As expected, the ascorbate oxidases are very closely related to each other. The bacterial proteins phenoxazinone synthase and the copper resistance gene product from *P. syringae* are very distant from the other proteins included in Table V. The rape Bp10 gene product exhibits significant similarity to ascorbate oxidase (about 72% differences).

The structurally based amino-acid sequence alignments and the analysis of the published (101) and presented similarity matrices suggest an evolutionary scheme for this group of proteins, which is shown in Fig. 9. The existence of a quasi-symmetrical arrangement of the N-terminal and C-terminal domains strongly suggests evolution by a duplication of a gene encoding a single protein domain of an ancestral small blue copper protein. The two domains in tandem might have

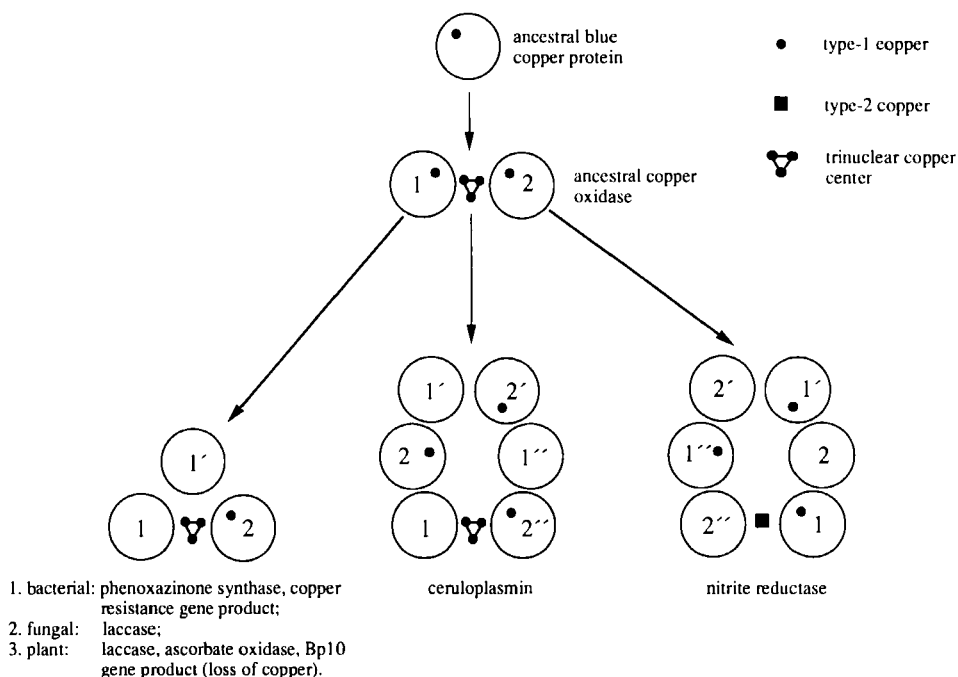


FIG. 9. An evolutionary scheme for the blue oxidases and related proteins.

functioned as a quasi-symmetrical oxidase with two type-1 copper sites after acquisition of a trinuclear copper site. The insertion of a third "single-domain" genetic element and the subsequent loss of type-1 coppers in domains 1 and 1' may have lead to the bacterial proteins penoxazinone synthase and the copper resistance gene product from *P. syringae*, to the fungal laccases, and to the plantal ascorbate oxidases, the laccases, and the rape Bp10 gene product. The rape Bp10 gene product lost all coppers during its evolution.

The pronounced threefold repeat in the six-domain molecule ceruloplasmin contradicts evolution by a duplication of an ascorbate oxidase-like molecule and suggests evolution from the tandem two-domain molecule by triplication, possibly before acquisition of the trinuclear copper site. This might have occurred later, between the N- and C-terminal domains.

The copper-containing nitrite reductase from *A. cycloclastes* may also have evolved from this ancestral oxidase. Nitrite reductase is a two-domain protein that functions as a trimeric molecule. During its evolution from the ancestral copper oxidase, a gene inversion must have occurred, so that domain 2 of the ancestral oxidase is now domain 1 of nitrite reductase. Domain 1 of the ancestral oxidase lost its type-1 copper but has become domain 2 in nitrite reductase after the gene inversion.

VIII. Oxidation-Reduction Potentials

Redox potentials for the different copper centers in the blue oxidases have been determined for all members of the group but in each case only for a limited number of species. The available data are summarized in Table VI (120, 121). The redox potentials for the type-1 copper of tree laccase and ascorbate oxidase are in the range of 330–400 mV and comparable to the values determined for the small blue copper proteins plastocyanin, azurin, and cucumber basic protein (for redox potentials of small blue copper proteins, see the review of Sykes (122)). The high potential for the fungal *Polyporus* laccase is probably due to a leucine or phenylalanine residue at the fourth coordination position, which has been observed in the amino-acid sequences of fungal laccases from other species (see Table IV and Section V.B). Two different redox potentials for the type-1 copper were observed for human ceruloplasmin (105). The 490-mV potential can be assigned to the two type-1 copper sites with methionine ligand and the 580-mV potential to the type-1 center with the isosteric leucine at this position (see Section V.B). The

TABLE VI

 OXIDATION-REDUCTION POTENTIALS OF THE COPPER CENTERS OF BLUE
 COPPER OXIDASES

Protein	pH	Potential, E^0 (mV)			Reference
		Type 1	Type 2	Type 3	
Laccase					
Fungal					
<i>Polyporus</i>	5.5	785	—	782	(120)
+ 1 mM NaF	5.5	780	—	570	
Tree					
<i>Rhus</i>	7.5	394	365	434	(120, 121)
+ 10 mM NaF	7.5	390	390	390	
+ Fe(CN) ⁴⁻	7.5	434	—	483	
Ascorbate oxidase					
<i>Cucurbita pepo medullosa</i>	7.0	344 ^a	—	344 ^a	(18)
	7.0	327 ^b	—	357 ^b	
<i>Cucumis sativus</i>	6.0	350	—	—	(71)
Ceruloplasmin					
Human	5.5	490, 580	—	—	(105)

^a At 25°C.^b At 10°C.

redox potentials for the type-3 centers are equal to or somewhat higher than the respective type-1 potentials. For ascorbate oxidase a difference of +30 mV between the type-3 and the type-1 potentials was observed when they were determined at 10°C in contrast to 25°C, where no distinction was possible (18). It is intriguing that the type-3 potential in fungal laccase is also greater, which is necessary for its enzymatic function (the reason for this will be discussed later). It will be interesting to learn what structural changes, compared with tree laccase or ascorbate oxidase, are required to give this elevation of redox potential once the X-ray structures of a fungal and tree laccase have been determined. Redox potentials for the type-2 site have been reported only for tree laccase. They had to be determined from a redox titration of the type-2 EPR signal. The values obtained do not differ much from those of the other copper centers. Taking into account that an integral trinuclear copper site is present in the blue oxidases and that there are no separated type-2 and type-3 centers makes it more plausible to define a unique redox potential for this trinuclear copper species. The type-2 EPR signal and the 330-nm band are both spectroscopic signals

of this copper species. Redox titrations using one of these signals should give the same results for the redox potential.

IX. Kinetic Properties of Laccase and Ascorbate Oxidase

Numerous studies concerning the catalytic and binding properties of the blue oxidases are well documented in the formerly mentioned reviews (see, for example, for laccase (10), for ascorbate oxidase (19), and for ceruloplasmin (26)). Important data, concentrating on laccase and ascorbate oxidase only, are summarized here.

Results from steady-state kinetics for laccase and ascorbate oxidase are given in Table VII. Listed are k_{cat} , K_m , and k_{cat}/K_m values at different pH values. The k_{cat}/K_m values indicate the low limit of the bimolecular enzyme-substrate reaction rate. The most reactive reducing substrate for tree laccase is hydroquinone with $k_{\text{cat}} = 2.4 \times 10^2 \text{ sec}^{-1}$, $K_m = 2.0 \times 10^{-1} M$, and $k_{\text{cat}}/K_m = 1.2 \times 10^3 M^{-1} \text{ sec}^{-1}$ and for ascorbate oxidase, ascorbate with $k_{\text{cat}} = 7.5 \times 10^3 \text{ sec}^{-1}$, $K_m = 2.0 \times 10^{-4} M$, and $k_{\text{cat}}/K_m = 3.8 \times 10^7 M^{-1} \text{ sec}^{-1}$. The data do not show a remarkable pH dependence.

A "ping-pong di Theorell-Chance" mechanism has been deduced for tree laccase from steady-state kinetics (123). This mechanism is characterized by the sequential entry of the two substrates and the immediate

TABLE VII
STEADY-STATE KINETICS OF LACCASE AND ASCORBATE OXIDASE

Enzyme	Substrate	pH	k_{cat} (sec^{-1})	K_m (M)	k_{cat}/K_m ($M^{-1} \text{ sec}^{-1}$)	Reference
Laccase	Ascorbate	6.0	1.5	1.0×10^{-2}	1.5×10^2	(19)
<i>Rhus</i>	$\text{Fe}(\text{CN})_6^{4-}$	6.0	2.0×10^1	5.0×10^{-2}	4.0×10^2	(19)
<i>vernificera</i>	Ascorbate	7.5	8.2	5.9×10^{-2}	1.4×10^2	(19)
	Hydroquinone	7.5	2.4×10^2	2.0×10^{-1}	1.2×10^3	(123)
	Oxygen	7.5	1.3×10^2	2.1×10^{-5}	6.1×10^6	(123)
<i>Rhus succedanea</i>	Ascorbate	6.0	3.0×10^1	1.7×10^{-2}	1.8×10^3	(19)
	$\text{Fe}(\text{CN})_6^{4+}$	6.0	2.2×10^2	2.2×10^{-2}	1.0×10^4	(19)
	Ascorbate	7.5	8.8×10^1	6.0×10^{-3}	1.5×10^4	(19)
	$\text{Fe}(\text{CN})_6^{4+}$	7.5	7.8×10^1	1.1×10^{-2}	7.1×10^3	(19)
Ascorbate oxidase	Ascorbate	6.0	7.5×10^3	2.0×10^{-4}	3.8×10^7	(19)
<i>Cucurbita pepo</i>	$\text{Fe}(\text{CN})_6^{4-}$	6.0	2.5×10^1	3.0×10^{-3}	8.3×10^3	(19)
<i>medullosa</i>	Ascorbate	7.5		Unaffected by pH		(19)
	$\text{Fe}(\text{CN})_6^{4-}$	7.5	1.7	5.0×10^{-3}	8.5×10^2	(19)

release of the respective products. The actual catalytic cycle will consist of very different steps but the finding that the two substrates react in a ping-pong mechanism is important.

Transient kinetics such as stopped flow, pulse radiolysis, or laser-flash photolysis has been applied to monitor the different steps during the catalytic cycle. In the presence of both substrates, complex patterns that are difficult to interpret have been obtained. Therefore, transient kinetics was carried out in the presence of only one substrate in each case. One process that has been investigated is the anaerobic reduction of the enzyme. A second is the reoxidation of the reduced enzyme by dioxygen. Results of the anaerobic reduction of laccase and ascorbate oxidase are given in Table VIII. The reduction of the type-1 copper, monitored by the bleaching of the 600-nm band, is a bimolecular second-order reaction. The reaction is biphasic for tree laccase and ascorbate oxidase with hydroquinone and reductase as substrates, respectively, and it is monophasic in the other cases. The rate constants for tree laccase with hydroquinone as a substrate are in the range of 2.0×10^2 to $2 \times 10^4 M^{-1} \text{ sec}^{-1}$ with ascending values from pH 6.5 to pH 8.5 (124). The values for fungal laccase are three to four orders of magnitudes higher (125). The rates for ascorbate oxidase with reductate as a substrate are about $10^4 M^{-1} \text{ sec}^{-1}$ and exhibit no remarkable pH dependence (18). Reaction of one-electron-reduced nitroaromatics (ArNO_2^-) gives rate constants of $<2 \times 10^6 M^{-1} \text{ sec}^{-1}$ for tree laccase (126) and $(1-3) \times 10^7 M^{-1} \text{ sec}^{-1}$ (127) for ascorbate oxidase. Ascorbate as a substrate for ascorbate oxidase should be at least as fast as the given rate constants since the reaction is completed within the dead-time of the stopped flow instrument, 3 to 5 msec (18). Recent studies on ascorbate oxidase using laser-flash photolysis (128) or pulse radiolysis (129, 130) reveal rate constants for the radicals of lumiflavin, deazaflavin, CO_2^- and MV^+ between 10^7 and $10^9 M^{-1} \text{ sec}^{-1}$. The pH dependence was not determined. The data suggests that the type-1 copper is the primary electron receptor from the reducing substrate. In the case of ascorbate oxidase with ascorbate as a substrate, it has been shown that one electron is transferred from ascorbate and that the generated semidehydroascorbate spontaneously dismutates in solution (131).

The anaerobic reduction of the trinuclear copper species monitored by the bleaching of the 330-nm band, the reappearance of the 600-nm band, and the disappearance of the type-2 EPR signal appear to be multiphasic processes in most cases. For fungal laccase, the process is monophasic with a unimolecular rate constant of 1.0 sec^{-1} (125). Tree laccase with hydroquinone as a substrate (124) displays a pH depen-

TABLE VIII

ANAEROBIC REDUCTION OF LACCASE AND ASCORBATE OXIDASE

Kind of type-1 copper reduction and rate (~610 nm)						Kind of type-2 and type-3 copper reduction and rate (~330 nm and/or reappearance of the 610-nm band)						
Enzyme	Substrate	pH	K_{init} ($M^{-1} \text{ sec}^{-1}$)	K_2 ($M^{-1} \text{ sec}^{-1}$)	Reference	Substrate	pH	K_{init} ($M^{-1} \text{ sec}^{-1}$)	K_1 (sec $^{-1}$)	K_2 (sec $^{-1}$)	K_3 (sec $^{-1}$)	Reference
Laccase												
Fungal	Hydroquinone	5.5	1.7×10^7	—	(125)	Hydroquinone	5.5	—	—	—	1.0	(125)
<i>Polyporus versicolor</i>	$\text{Fe}(\text{CN})_6^{4-}$	5.5	1.5×10^6	—	(125)	Ascorbate	5.5	—	—	—	1.0	(125)
						Inactive form already at pH 5.5; OH^- binds to type-2 copper						
Tree	Hydroquinone	6.5	3.6×10^2	1.6×10^2	(124)	Hydroquinone	6.5	4.0×10^2	—	—	—	(124)
<i>Rhus vernicifera</i>	Hydroquinone	7.4	1.6×10^3	8.0×10^2	(124)	Hydroquinone	7.4	1.5×10^3	—	—	0.4	(124)
	Hydroquinone	8.5	1.8×10^4	4.0×10^3	(124)	Hydroquinone	8.5	8.0×10^3	—	—	0.25	(124)
	ArNO_2^-	7.4	$<2 \times 10^6$	—	(126)	CO_2^-	7.0	—	—	—	1.0	(132)
						Inactive form at high pH; OH^- binds to type-2 copper						
Ascorbate oxidase	Reductate	6.1	2.2×10^4	1.2×10^4	(18)	Reductate	6.1	—	100	—	—	(18)
<i>Cucurbita pepo</i>	Reductate	7.0	1.7×10^4	1.0×10^4	(18)	Reductate	7.0	—	100	—	—	(18)
<i>medullosa</i>	Reductate	7.8	1.4×10^4	0.8×10^4	(18)	Reductate	7.8	—	100	—	—	(18)
	Ascorbate	Much faster, reaction within the			(18)	Rapid freeze-quench EPR experiments indicate that type-2 copper is						(18)
						reduced more slowly						
	ArNO_2^-	7.5	$1-3 \times 10^7$	—	(127)							
	Lumiflavin ^a	7.0	2.7×10^7	—	(128)							
		7.0	3.8×10^7	—	(120)	Lumiflavin ^a	7.0	—	97	—	2.4	(129)
	CO_2^-	7.0	1.2×10^9	—	(130)	CO_2^-	7.0	—	201	20	2.3	(130)
		7.0	1.1×10^9	—	(129)		7.0	—	120	—	2.0	(129)
	MV^+	7.0	2.6×10^7	—	(129)	MV^+	7.0	—	127	—	2.3	(129)
	Deazaflavin ^a	7.0	1.5×10^8	—	(129)	Deazaflavin ^a	7.0	—	121	—	2.5	(129)

^a Radical form.

dence with a bimolecular reaction ($k_{\text{init}} = 4.0 \times 10^2 \text{ M}^{-1} \text{ sec}^{-1}$) at pH 6.5 and a biphasic behavior at pH 7.4 and 8.5. The first reaction is a bimolecular second-order reaction with increasing rate constants at ascending pH. The second one is a unimolecular reaction with rate constants of about 0.3 sec^{-1} . Pulse radiolysis studies on tree laccase with the $\text{CO}_2^{\cdot -}$ radical as a substrate at pH 7.0 reported a monophasic reaction ($k = 1.0 \text{ sec}^{-1}$) (132). The disappearance of the type-2 EPR signal has been determined for tree laccase by rapid freeze-quench experiments (133). It is as fast as the reduction of the type-1 copper. Tree laccase is inactive at high pH. Because the type-2 EPR signal is altered, it has been concluded that an OH^- binds to the type-2 copper, causing inactivation of the enzyme.

The anaerobic reduction of the trinuclear copper center for ascorbate oxidase with different substrates presents a distinct picture. The reaction with reductate is monophasic with a unimolecular rate constant of 100 sec^{-1} (18), independent of pH. Rapid freeze-quench EPR experiments indicate that the type-2 EPR signal vanishes more slowly (18). The pulse radiolysis studies of the radicals of lumiflavin, deazaflavin, $\text{CO}_2^{\cdot -}$, and $\text{MV}^{\cdot +}$ at pH 7.0 (129, 130) showed a biphasic behavior with an initial, faster reaction ($k = 97\text{--}127 \text{ sec}^{-1}$) and a final, slower reaction ($k \sim 2 \text{ sec}^{-1}$) (129). Different results have been obtained by Farver and Pecht (130) with $\text{CO}_2^{\cdot -}$ as a substrate. They found a triphasic reaction with unimolecular rate constants $k = 201 \text{ sec}^{-1}$, $k_2 = 20 \text{ sec}^{-1}$, and $k_3 = 2.3 \text{ sec}^{-1}$. The first constant is twice that in a study by Kyritsis *et al.* (129), whereas the third constant is identical. The second constant was not observed in the study.

The unimolecular reduction of the trinuclear copper center is caused by intramolecular electron transport from the type-1 copper to the trinuclear copper species. The turnover numbers represented by the k_{cat} values (see Table VII) are one to two orders of magnitudes greater than the observed intramolecular electron transfer rate constants. They should be at least as large as the turnover numbers. The low rates seem to imply that the enzymes are in an inactive form under the conditions of the anaerobic reduction experiments. It will be shown later that there is experimental evidence for this assumption.

The reoxidation studies on laccase and ascorbate oxidase are listed in Table IX. The reoxidation of the type-1 copper and of the trinuclear copper site occurs at a rate of $5 \times 10^6 \text{ M}^{-1} \text{ sec}^{-1}$ both for tree laccase (134) and for ascorbate oxidase (135). During reoxidation with H_2O_2 , an O_2^{2-} intermediate is formed in several minutes, which is documented for tree laccase by changes in the CD spectrum (136) and for ascorbate oxidase in the formation of an absorption band at 350 nm

TABLE IX
 REOXIDATION OF REDUCED ENZYME

Enzyme	Oxidant	Signal of intermediate	Putative intermediate	Rate of reoxidation	Rate of decay of intermediate	Reference
Laccase <i>Polyporus versicolor</i>	O ₂	Absorption maximum at 360 nm, new EPR signal at low temperature (10 K)	O ⁻ radical	615-nm band, $5 \times 10^6 M^{-1} \text{sec}^{-1}$; 330-nm band, $5 \times 10^6 M^{-1} \text{sec}^{-1}$; 360-nm absorption maximum, $5 \times 10^6 M^{-1} \text{sec}^{-1}$; type-2 copper EPR signal, 20-s halftime	Absorption maximum at 360 nm, 20-s halftime, first-order reaction	(134)
TlHg derivative	O ₂	Absorption bands at 340 and 470 nm, CD changes in 500- to 1000-nm range, disappearance of MCD signal at 730 nm	HO ₂ ⁻	340- and 470-nm bands, ^a $2 \times 10^6 M^{-1} \text{sec}^{-1}$	Formation is irreversible	(138)
	H ₂ O ₂	CD changes in 250- to 300-nm range	O ₂ ²⁻	CD changes, formation in <10 min	New CD spectrum stable at >6 hr	(136)
Ascorbate oxidase <i>Cucurbita pepo medullosa</i>	O ₂	No data	No data	610-nm band, $5 \times 10^6 M^{-1} \text{sec}^{-1}$; 330-nm band, $5 \times 10^6 M^{-1} \text{sec}^{-1}$	No data	(135)
	H ₂ O ₂	Absorption band at 350 nm, pH 7.6	O ₂ ²⁻	350-nm band formation in several minutes	350-nm band decay over several hours	(137)

^a Measured at 3°C.^b Addition to oxidized enzyme in equimolar amounts.

(137). The intermediates are stable for several hours in both enzymes. An interesting intermediate was found during reoxidation of fully reduced tree laccase by dioxygen (134). This intermediate caused the rapid formation of an absorption maximum at 330 nm and also affected the type-2 copper EPR signal. It decayed in a first-order reaction with a half-time of 20 sec. A new EPR signal at a low temperature (10 K) due to this radical could be detected. This radical has been described as an O⁻ radical. Recently, Solomon and co-workers (97, 138, 139) have identified and spectroscopically characterized an oxygen intermediate during the reaction of either fully reduced native tree laccase or TlHg-laccase with dioxygen. The intermediate has been described as a hydroperoxide binding as 1,1- μ between either CU2 and CU4 or CU3 and CU4.

From these data, it follows that the dioxygen binds to the trinuclear copper site. This species may store three electrons and transfer them to the bound dioxygen followed by a final one-electron transfer.

From the smoothed van der Waals surface (Conolly surface) calculated for the X-ray structure model of ascorbate oxidase, a binding pocket for the reducing substrate near the type-1 copper and two channels providing access to the trinuclear copper species could be identified (74). The binding pocket for the reducing substrate is complementary to an ascorbate molecule. The channel giving access to copper atoms CU2 and CU3 of the trinuclear site is much broader than the channel leading to CU4. The former is the main channel for the entrance of the dioxygen and protons and the release of the water molecules. Figures and a detailed description of the pocket and the channels are given in Messerschmidt *et al.* (74).

X. Functional Derivatives

A. GENERAL REMARKS

The blue oxidases may be inhibited by a number of different substances. For ceruloplasmin, there are systematic studies showing that two groups of more specific inhibitors exist: (1) halides and inorganic anions and (2) carboxylate ions (140–143). The rank of inhibition effects of anions with ceruloplasmin is $\text{CN}^- > \text{N}_3^- > \text{OCN}^- > \text{SCN}^- > \text{SeCN}^- > \text{F}^- > \text{I}^- \approx \text{NO}_3^- \approx \text{Cl}^- > \text{Br}^- > \text{ClO}_4^-$, tetraborate, borate, phosphate, sulfate, and cacodylate (141). Inhibition by CN^- , N_3^- , and F^- has been investigated predominantly with laccase (133, 144, 145) and ascorbate oxidase (146). The order of inhibitory action is the same as that observed for ceruloplasmin. Inhibition by these anions appears to be quite satisfactory. Strong binding to the spectroscopic type-2 copper is indicated by a perturbation of the EPR signal of this site.

Laccases also become inhibited at higher pH values. Tree laccase is inhibited above pH 6.5. It appears that at pH 7.4 ~50% of the enzyme molecules are inhibited due to the binding of OH^- to the type-2 copper. The nature of this OH^- binding to the resting form of ascorbate oxidase will be demonstrated below.

The reaction of nitric oxide with laccase (76) and ascorbate oxidase (147) has been studied as well. Nitric oxide fully reduces fungal and tree laccase when it is added to the oxidized enzyme under anaerobic conditions. In addition the binding of one NO molecule to laccase can be detected. This is characterized by a new EPR signal and has been described as coordinated with the type-2 copper (76). Only the reduction of the type-1 copper has been observed when NO has been added to ascorbate oxidase under anaerobic conditions.

Other functional derivatives have been prepared. Two of them deserve special mention, namely the type-2 copper depleted (T2D) enzyme and a derivative in which the type-1 copper is replaced by mercury (T1Hg). The T2D derivative will be dealt with in a special paragraph. The T1Hg form was originally prepared by McMillin and co-workers (148) from tree laccase. This derivative lacks the type-1 copper EPR signal and makes possible the recording of the type-2 EPR signal alone. It has been used to study the reaction of dioxygen with the reduced derivative (138). As already mentioned, the formation of an oxygen intermediate could be observed. This intermediate was bound irreversibly to the trinuclear copper site due to abortion of further reduction of the dioxygen caused by the lack of the type-1 copper redox center. The preparation of the apoenzyme and reconstitution are possible for all three blue oxidases (see for laccase (10), for ascorbate oxidase (19), and for ceruloplasmin (26)).

X-ray crystal structures of four functional derivatives of ascorbate oxidase were determined (149, 150). The results of these investigations and implications for the catalytic mechanism of the blue oxidases will be outlined in the next section.

B. X-RAY STRUCTURE OF THE TYPE-2 DEPLETED (T2D) FORM OF ASCORBATE OXIDASE

It has been demonstrated by several groups that copper can be selectively removed from the blue oxidases, causing a disappearance of the type-2 EPR signal. Several methods have been described for laccase from *P. versicolor* (151, 152) and from the Japanese lacquer tree, *Rhus vernicifera* (153–156), and for ascorbate oxidase from zucchini (156–158). All procedures except one involve working under reducing conditions with metal chelating reagents, such as EDTA, dimethyl glyoxime, bathocuproine disulfonate, or nitrilotriacetate. Reaction of *N,N*-diethyldithiocarbamate with ascorbate oxidase under aerobic conditions in solution gave the type-2 depleted enzyme (158). Many experiments were carried out on T2D multicopper oxidases in the past and to interpret these experiments it is important to know the actual occupation of the copper sites in the depleted enzyme. An X-ray structure analysis of the depleted enzyme of ascorbate oxidase (149) provided new information on this point.

Crystals of native oxidized ascorbate oxidase were anaerobically dialyzed in microcells against 50 mM sodium phosphate buffer, pH 5.2, containing 25% (v/v) methylpentanediol (MPD), 1 mM EDTA, 2 mM dimethyl-glyoxime (DMG), and 5 mM ferrocyanide for 7 and 14 hr.

Thereafter, crystals were brought back to the aerobic 25% MPD solution, buffered with 50 mM sodium phosphate, pH 5.5. This procedure is based on Avigliano *et al.*'s (157) method of preparing T2D ascorbate oxidase in solution and was modified by Merli *et al.* (159) for use with ascorbate oxidase crystals. The 2.5-Å-resolution X-ray structure analysis by difference-Fourier techniques and crystallographic refinement shows that about 1.3 copper ions per ascorbate oxidase monomer are removed. The copper is lost from all three copper sites of the trinuclear copper species, whereby the EPR-active type-2 copper is the most depleted (see Fig. 10). Type-1 copper is not affected. The EPR spectra from polycrystalline samples of the respective native and T2D ascorbate oxidase were recorded. The native spectrum exhibits the type-1 and type-2 EPR signals in a ratio of about 1 : 1, as expected from the crystal structure. The T2D spectrum reveals the characteristic resonances of the type-1 copper center, also observed for T2D ascorbate oxidase in frozen solution, and the complete disappearance of the spectroscopic type-2 copper. This observation indicates preferential formation of a Cu-depleted form with the holes equally distributed over all three copper sites. Each of these Cu-depleted species may represent an anti-ferromagnetically coupled copper pair that is EPR-silent and that could explain the disappearance of the type-2 EPR signal.

C. X-RAY STRUCTURE OF THE REDUCED FORM OF ASCORBATE OXIDASE

Crystals of the reduced form (REDU) of ascorbate oxidase (150) had to be prepared and mounted in a glass capillary in a glove box that was flushed with argon gas and operated with a slight overpressure of argon. The degassed buffer solution was stored in the glove box. Dithionite was added to the buffer solution to a concentration of 10 mM. The siliconised X-ray capillary was washed with the buffer. The crystals were soaked in the reducing buffer for half an hour. After 15 min, the crystals lost their blue color. They were mounted in the X-ray capillary and carefully sealed with wax that had been degassed in the desiccator. Crystals mounted in this way remained colorless and reduced over weeks.

A 2.2-Å resolution X-ray structure analysis by difference-Fourier techniques and crystallographic refinement delivered the following results (150). The geometry at the type-1 copper remains much the same compared with the oxidized form. The mean copper-ligand bond lengths of both subunits increased by 0.04 Å on average, which is insignificant but may indicate a trend. Similar results have been ob-

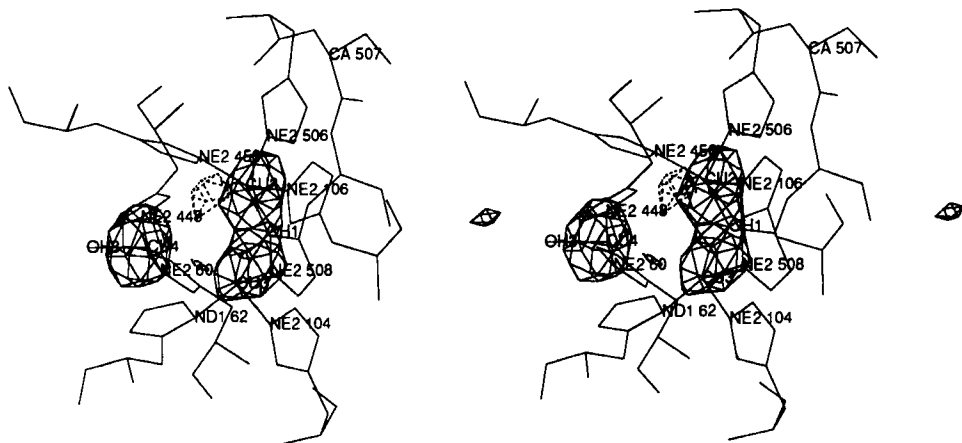


FIG. 10. Averaged $FO_{T2D}-FC_{T2D}$ difference electron density map plus atomic model around the trinuclear copper site. Contour levels: -18.0 , solid line; 18.0 , dashed line. Magnitudes of the hole are less than -35.0 .

tained for the reduced forms of poplar plastocyanin at pH 7.8 (160), azurin from *Alcaligenes denitrificans* (161), and azurin from *P. aeruginosa* (162). In reduced poplar plastocyanin at pH 7.8 a lengthening of the two Cu—N(His) bonds by about 0.1 \AA is observed. In reduced azurin, pH 6.0, from *A. denitrificans*, the distances from copper to the axial methionine and to the carbonyl oxygen each increase by about 0.1 \AA . The same shifts are found in the refined structures of reduced azurin from *P. aeruginosa* determined at pH values of 5.5 and 9.0 (162). The estimated accuracy of the copper–ligand bond lengths in the high-resolution structures of the above-mentioned small blue copper proteins is about 0.05 \AA . The type-1 copper sites in the small blue copper proteins as well as in ascorbate oxidase require little reorganization in the redox process.

A schematic drawing of the reduced form of ascorbate oxidase is shown in Fig. 11. The structural changes are considerable at the trinuclear copper site. Thus on reduction the bridging oxygen ligand OH1 is released and the two coppers, CU2 and CU3, move toward their respective histidines and become three coordinated, a preferred stereochemistry for Cu(I). The copper–copper distances increase from an average of 3.7 to 5.1 \AA for CU2—CU3, 4.4 \AA for CU2—CU4, and 4.1 \AA for CU3—CU4. The mean values of the copper–ligand distances of the trinuclear copper site are comparable to those of native oxidized ascorbate oxidase and binuclear copper model compounds with nitrogen

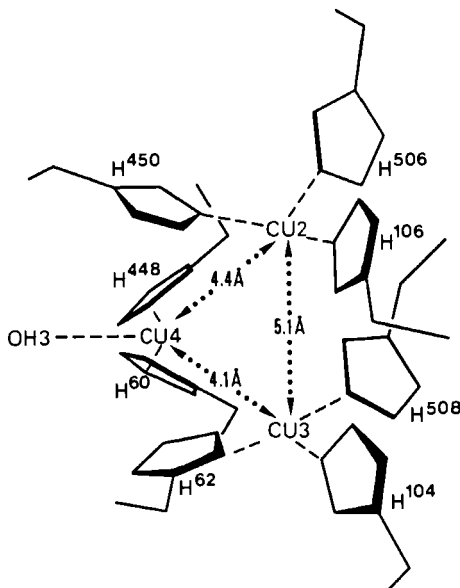


FIG. 11. Schematic drawing of the reduced form of ascorbate oxidase around the trinuclear copper site. The included copper-copper distances are the mean values between both subunits.

and copper ligands (98, 99). CU4 remains virtually unchanged between reduced and oxidized forms. Coordinatively unsaturated copper(I) complexes are reported in the literature. Linear two-coordinated (163) and T-shaped three-coordinated (164) copper(I) compounds have been reported. The copper nitrogen distances for both linearly arranged nitrogen ligands are about 1.9 Å, about 0.1 Å shorter than copper nitrogen bond lengths in copper(II) complexes. In T-shaped copper(I) complexes, the bond length of the third ligand is increased. Copper ion CU4 is in a T-shaped threefold coordination not unusual for copper(I) compounds. The structure of the fully reduced trinuclear copper site is quite different therefore from that of the fully oxidized resting form of the enzyme and its implications for the enzymatic mechanism will be discussed below.

D. X-RAY STRUCTURE OF THE PEROXIDE FORM OF ASCORBATE OXIDASE

Native crystals of ascorbate oxidase were soaked in harvesting buffer solution (50 mM sodium phosphate, 25% MPD, pH 5.5) containing

different H_2O_2 concentrations (150). Concentrations of H_2O_2 greater than 20 mM caused the crystals to crack, to become brownish, and finally to decompose within several hours depending on the concentration of H_2O_2 used. At 10 mM H_2O_2 , the crystals remained blue and did not crack at 1½ to 2 days. A native crystal was therefore soaked for 2 hr in 10 mM H_2O_2 containing harvesting buffer solution, mounted in the X-ray capillary, and immediately used for the X-ray intensity measurements.

The 2.6 Å resolution, X-ray structure analysis by difference-Fourier techniques and crystallographic refinement reveal the data illustrated in Fig. 12 (150). The geometry at the type-1 copper site is not changed compared with that of the oxidized form. The copper–ligand bond distances averaged for both subunits show no significant deviations from those of the oxidized form. As in the reduced form, the structural

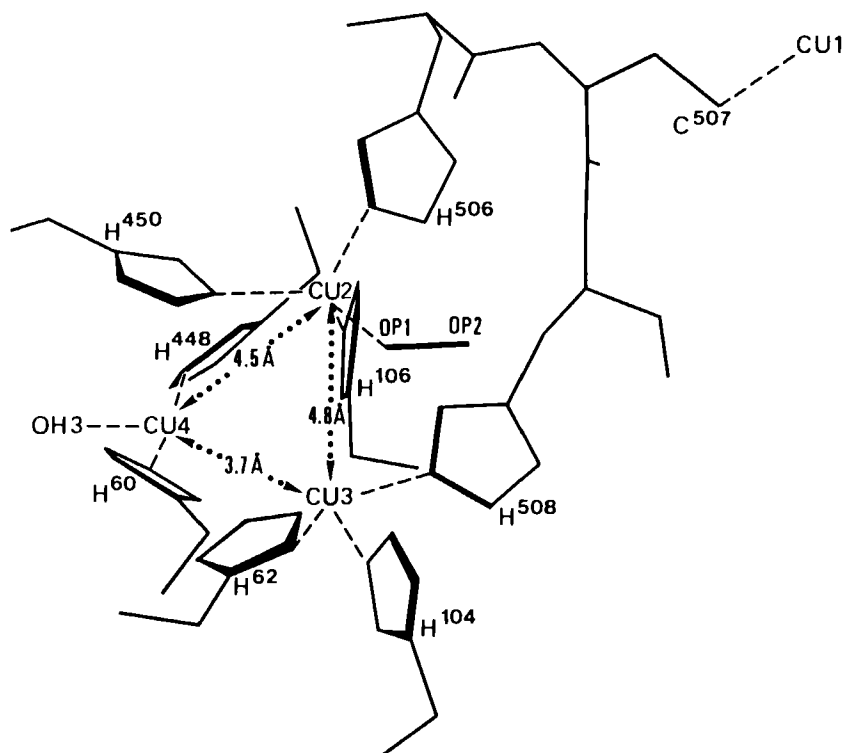


FIG. 12. Schematic drawing of the peroxide form of ascorbate oxidase around the trinuclear copper site. The included copper–copper distances are the mean values between both subunits.

changes are remarkable at the trinuclear copper site. The bridging oxygen ligand OH1 is absent, the peroxide binds terminally to the copper atom CU2 as hydroperoxide, and the copper–copper distances increase from an average of 3.7 to 4.8 Å for CU2–CU3 and 4.5 Å for CU2–CU4. The distance CU3–CU4 remains at 3.7 Å. The mean values of the copper–ligand distances of the trinuclear copper site are again comparable to those of native oxidized ascorbate oxidase and corresponding copper model compounds.

Copper ion CU3 is threefold coordinated as in the reduced form but the coordination by the ligating N atoms of the corresponding histidines is not exactly trigonal–planar and the CU3 atom is at the apex of a flat trigonal pyramid. The coordination sphere around CU4 is not affected and is similar in all three forms. Copper atom CU2 is fourfold coordinated to the NE2 atoms of the three histidines, as in the oxidized form, and by one oxygen atom of the terminally bound peroxide molecule in a distorted tetrahedral geometry. Its distance to CU3 increases from 4.8 Å in the oxidized peroxide derivative to 5.1 Å in the fully reduced enzyme. The bound peroxide molecule is directly accessible from the solvent, through a channel leading from the surface of the protein, and to the CU2–CU3 copper pair. This channel has already been described earlier and its possible role as a dioxygen transfer channel has been discussed. An interesting feature is the close proximity of the imidazole ring of histidine 506 to the peroxide molecule. Histidine 506 is part of one possible electron transfer pathway from the type-1 copper to the trinuclear copper site and could indicate a direct electron pathway from CU1 to dioxygen. It may also help to stabilize important intermediate states in the reduction of dioxygen.

The strong positive peaks at CU2 in both $\text{FO}_{\text{NATI}}\text{--FO}_{\text{PEOX}}$ and $\text{FO}_{\text{REDU}}\text{--FO}_{\text{PEOX}}$ electron density maps could not be explained by a shift of CU2 alone. Occupancies of the copper atoms, the oxygen atoms OH3, and the peroxide molecule were refined. Type-1 copper CU1 is almost not affected. Copper atoms CU3 and CU4 are only partly removed but copper atom CU2 is about 50% depleted. The oxygen ligands exhibit full occupancy. The treatment of crystals of ascorbate oxidase with hydrogen peroxide generates not only a well-defined peroxide binding but also a preferential depletion of copper atom position CU2. In the copper-depleted molecules the ligating histidine 106 adopts an alternative side chain conformation detected in the 2FO–FC map, calculated with the final peroxide derivative model coordinates. This map shows that histidine 106 moves away when copper atom CU2 is removed and opens the trinuclear site even more. From the T2D crystal structure of ascorbate oxidase, it is apparent that copper from all three metal

binding sites of the trinuclear copper species is removed in different amounts. The movement of the histidine 106 side chain could explain how this process is accomplished.

Copper depletion may also cause instability of the protein against hydrogen peroxide. Reaction of hydrogen peroxide with excess ascorbate oxidase in solution leads to a rapid degradation of the enzyme (67). This can be monitored in the UV/visible PEOX–NATI difference spectrum by a negative band at 610 nm and a positive band at 305 nm. Adding four equivalents of hydrogen peroxide per monomer ascorbate oxidase does not lead to enzyme degradation and gives a positive peak at 305 nm indicative of peroxide binding. Unfortunately, it was not possible to monitor a UV/visible spectrum of dissolved crystals after X-ray data collection because of the dissociation of the bound peroxide in solution.

The reaction of dioxygen with laccase or ascorbate oxidase was reviewed in Section IX and in Messerschmidt *et al.* (74), where the possible binding modes of dioxygen to binuclear and trinuclear copper centers are discussed. A novel mode of dioxygen binding to a binuclear copper complex was found in a compound synthesized by Kitajima *et al.* (165). The complex contains peroxide in the $\mu\text{-}\eta^2\text{:}\eta^2$ mode, i.e., side-on between the two copper(II) ions. Such a binding mode of dioxygen has been detected in the crystal structure of the oxidized form of *Limulus polyphemus* subunit II hemocyanin (166). However, the binding mode of dioxygen to the trinuclear copper site in the blue oxidases appears to be different, as can be seen from the X-ray structure of the peroxide derivative of ascorbate oxidase.

During its reaction with fully reduced laccase, dioxygen binds to the trinuclear copper species and three electrons are very rapidly transferred to it, resulting in the formation of an "oxygen intermediate" with a characteristic optical absorption near 360 nm (134, 167) and a broad low temperature EPR signal near $g = 1.7$ (168, 169). The type-1 copper is concomitantly reoxidized when the low-temperature EPR signal is formed. The oxygen intermediate decays very slowly ($t_{1/2} \sim 1$ to 15 sec), correlated with the appearance of the type-2 EPR signal (170).

Solomon and co-workers (97, 138, 139) have identified and spectroscopically characterized an oxygen intermediate during the reaction of either fully reduced native tree laccase or T1Hg-laccase with dioxygen. They concluded from their spectroscopic data that the intermediate binds as 1,1- μ hydroperoxide between either CU2 and CU4 or CU3 and CU4. As it is unlikely that the dioxygen migrates or rearranges coordination during reduction, Messerschmidt *et al.* (150) proposed that the binding site and mode determined for the peroxide derivative of

ascorbate oxidase is representative of all reaction intermediates of dioxygen and, by homology arguments, is in all blue oxidases. The relevance of this binding mode for the catalytic mechanism will be discussed later.

E. X-RAY STRUCTURE OF THE AZIDE FORM OF ASCORBATE OXIDASE

The azide derivative was obtained by soaking the native crystals in a harvesting buffer solution containing 50 mM sodium azide for 24 hr (150). Binding of azide was indicated by a change of color of the crystal from blue to brownish. After X-ray intensity data collection, the crystals were dissolved in a solution containing 50 mM azide, 5 mM phosphate buffer, pH 5.5, and 8% MPD and the UV/visible spectrum was recorded at room temperature.

The results of the 2.3-Å resolution X-ray structure analysis by difference-Fourier techniques and crystallographic refinement are depicted in Fig. 13 (150). The geometry at the type-1 copper site is not changed compared with that of the native form. The copper–ligand bond distances averaged for both subunits show no significant deviations from those of the native form. Again, the structural changes are large at the trinuclear copper site. The bridging oxygen ligand OH1 and water molecule 145 have been removed, CU2 moves toward the ligating histidines, and two azide molecules bind terminally to it. The copper–copper distances increase from an average of 3.7 to 5.1 Å for CU2—CU3 and 4.6 Å for CU2—CU4. The distance CU3—CU4 decreases to 3.6 Å. The mean values of the copper–ligand distances of the trinuclear copper site are again comparable to those of native ascorbate oxidase and corresponding copper model compounds.

The coordination of CU3 resembles that in the peroxide form. The threefold coordination by histidines is a very flat trigonal pyramid. The coordination sphere around CU4 is not affected. CU2 is fivefold coordinated to the NE2 atoms of the three histidines, as in the reduced form, and to the two azide molecules. The two azide molecules are terminally bound at the apexes of a trigonal bipyramid. Both azide molecules bind to the copper atom CU2, which is well accessible from the broad channel leading from the surface of the protein to the CU2—CU3 copper pair. It is not unexpected that the second azide molecule (az^2 in Fig. 13) binds similarly to the peroxide molecule, as azide is regarded as a dioxygen analogue. There is no bound azide molecule bridging either CU2 with CU4 or CU3 with CU4.

The binding of azide to laccase as well as to ascorbate oxidase has been studied extensively by Solomon and co-workers (79, 80, 97, 171)

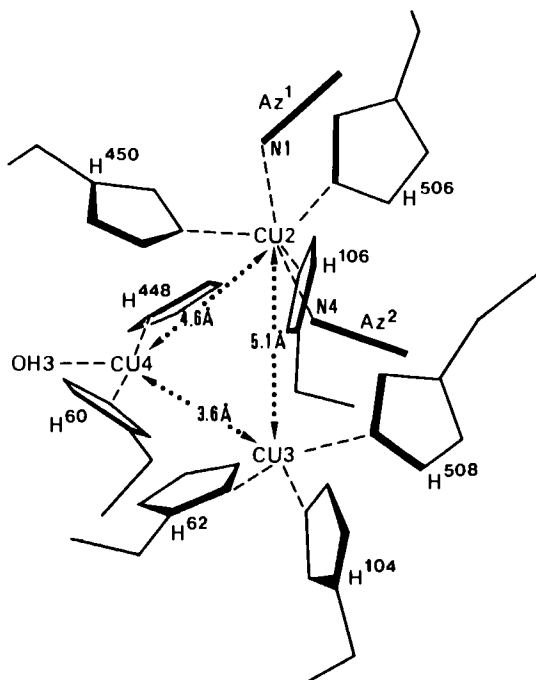


FIG. 13. Schematic drawing of the azide form of ascorbate oxidase around the trinuclear copper site. The included copper-copper distances are the mean values between both subunits.

and by Marchesini and associates (172, 173) by spectroscopic techniques. The derived spectroscopic models involve the binding of two azide ions to laccase and three to ascorbate oxidase with different affinities. As the binding of the high-affinity azide seems to generate spectral features related to the type-2 and type-3 coppers, the spectroscopic data were interpreted as the binding of at least one azide as a 1,3- μ bridge between the type-3 copper ions and the type-2 copper ion.

After the X-ray data collection for the azide derivative, the crystal was dissolved in azide-containing buffer and a UV/visible spectrum was recorded to check the spectral properties of the sample (150). The spectrum was characterized by a broad increase of absorption in the 400- to 500-nm region and an intense absorption maximum at 425 nm, very similar to the results of Casella *et al.* (172).

There are many structural studies of copper coordination compounds with azide ligands, mainly of mononuclear and binuclear copper complexes but a few also of trinuclear copper complexes. A comprehensive

review on copper coordination chemistry has been written by Hathaway (174). Azide binds only terminally to mononuclear systems. Fivefold coordination of nitrogen ligands including azide to Cu^{2+} is frequently found to be arranged as a trigonal bipyramid. In binuclear systems azide may bind terminally as 1,1- μ or bridging as 1,3- μ . Similarly two azides may bind di-1,1- μ or di-1,3- μ . Interaction with all three copper ions of a trinuclear complex may be either terminal as 1,1,1- μ or bridging as 1,1,3- μ . In the X-ray crystal structure of ascorbate oxidase two azide molecules bind terminally to the type-3 CU2. Azide binding in ascorbate oxidase resembles therefore the binding of azide to an isolated copper ion. In fact there is little interaction of CU2 with CU3 and CU4, which are 5.1 and 4.6 Å away, respectively.

The coordination of copper ion CU4 in the native oxidized structure is of some interest. It has only three ligating atoms at close distances, forming a T-shape coordination that is known for Cu(I) complexes (see discussion of the reduced form). However, the ligand field is completed if we take into account the π -electron systems of the imidazole rings of histidines 62 and 450 (see Fig. 6). A ligand field with tetragonal-pyramidal symmetry around CU4 is then formed. The shortest distances of CU4 are to CD2 450 with 3.4 Å and to CG 62 with 3.6 Å. These distances are too long for strong copper- π -electron interactions but the histidines will contribute to the CU4 ligand field.

XI. The Catalytic Mechanism

Catalytic reaction schemes for laccase and ceruloplasmin have been formulated on the basis of the mechanistic studies and the state of characterization of the copper redox centers at this time. They are outlined in the reviews on laccase by Reinhammar (10) and on ceruloplasmin by Rydén (26). The degree of correctness of these reaction schemes is rather limited due to the fact that the structure and spatial arrangement of the copper centers were unknown at this time.

A tentative catalytic mechanism of ascorbate oxidase has been proposed based on the refined X-ray structure and on spectroscopic and mechanistic studies of ascorbate oxidase and the related laccase. The results of these studies have been discussed in detail (74). The X-ray structure determinations of the fully reduced and peroxide derivatives define two important intermediate states during the catalytic cycle. A proposal for the catalytic mechanism incorporating this new information is given in Messerschmidt *et al.* (150) and presented in Fig. 14. This scheme should be valid in principle also for laccase due to the close similarities of both blue oxidases.

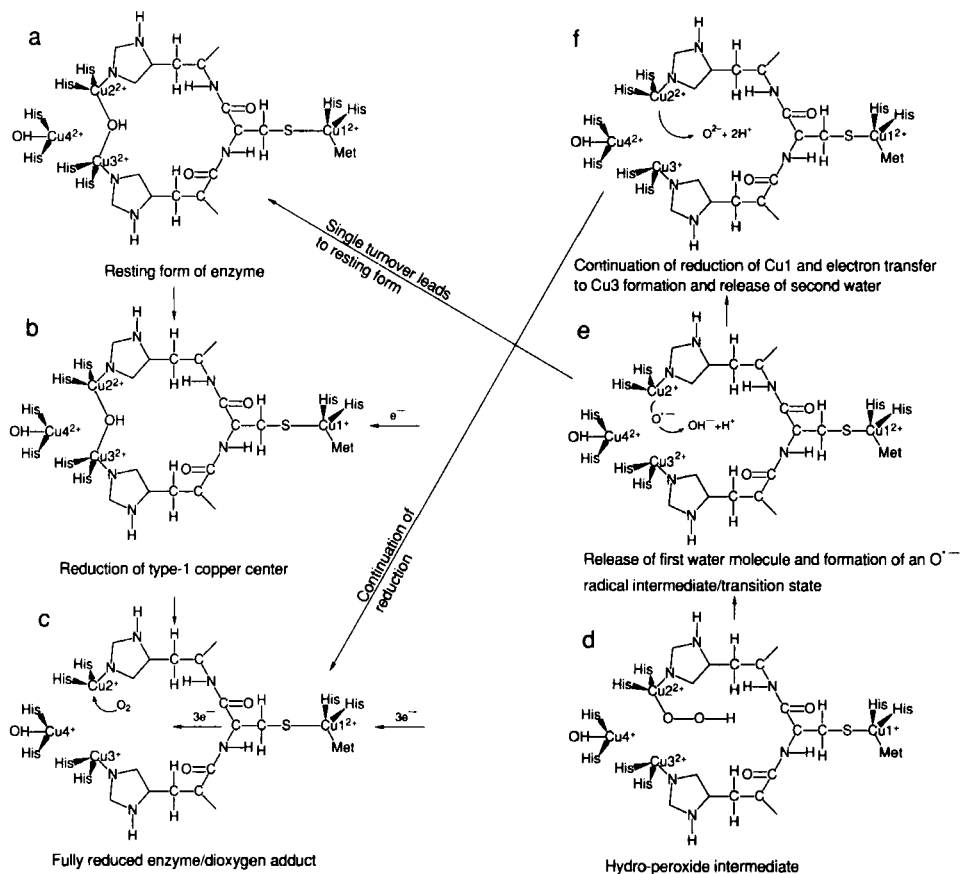


FIG. 14. Proposal for the catalytic mechanism of ascorbate oxidase.

The catalytic cycle starts from the resting form (Fig. 14a), in which all four copper ions are oxidized and CU2 and CU3 are bridged by an OH⁻ ligand. CU2 and CU3 are most likely the spin-coupled type-3 pair of copper and CU2 is the type-2 copper. The first step is the reduction of the type-1 copper CU1 by the reducing substrate in a one-electron transfer step (Fig. 14b). The electrons are transferred through the protein to either CU2 or CU3. Electron transfer may be through-bond, through-space, or a combination of both. A branched through-bond pathway is available, leading to CU2 with 9 bonds (including a hydrogen bond) and to CU3 with 11 bonds, respectively. The fully reduced enzyme requires four electrons to be transferred (Fig. 14c). Its structure was described in a previous section. The hydroxyl bridge between the

copper pair has been released and the distance from copper atom CU2 to CU3 has been increased to about 5.1 Å. Considerable reorganization energy will be necessary to reach this state from the resting form of the enzyme. At this stage, dioxygen may bind to the enzyme at CU2, probably in the manner shown in the peroxide derivative described in the appropriate section. A transfer of two electrons from the copper pair to dioxygen leads to the formation of a hydroperoxide intermediate (Fig. 14d). A third electron may be transferred from CU4 to the hydroperoxide intermediate, and a fourth electron from the type-1 copper to copper ion CU2. The O—O bond is broken at this stage and the first water molecule released (Fig. 14e). An oxygen radical has been detected in laccase by EPR. The EPR spectrum indicates that the type-1 copper has been reoxidized and that the EPR signals of the oxygen radical intermediate and type-1 copper are present. The CU2 is in the reduced state, whereas the oxidized copper atoms CU3 and CU4 may be spin-coupled and EPR silent. The reduced CU2 may facilitate O—O bond breakage and release of water. The catalytic cycle is continued by a further reduction of the type-1 copper center by the reducing substrate. This electron may be transferred to CU3 of the copper pair via the 11 bond pathway. Now, the fourth electron may be transferred to the oxygen radical intermediate from copper atom Cu2 and the second water molecule released (Fig. 14f). In the case of only four electron equivalents, the reaction may lead to the resting form and the second water may remain bound as the bridging ligand between CU2 and CU3, concomitant with a substantial rearrangement within the trinuclear copper site and its coordinating ligands. If turnover is continued, this will not occur and the trinuclear copper site may maintain a structure very close to that found in the fully reduced form. Only minor rearrangements will take place at the trinuclear copper site during the catalytic cycle, a prerequisite for facile electron transfer reactions. The four protons required for the formation of the two water molecules from dioxygen may be supplied from bulk water through the dioxygen channel via the water molecules bound in the vicinity of CU2 and CU3.

XII. Electron Transfer Processes

A. ELECTRON TRANSFER TO THE TYPE-1 COPPER REDOX CENTER

As previously mentioned, the electron transfer from one-electron-reduced nitroaromatics (ArNO_2^-), CO_2^- , methyl viologen $^{+}$, lumiflavin, or deazaflavin to the type-1 copper center (see Table VIII) takes

place in a bimolecular second-order reaction with rates compatible with or higher than the turnover number, with ascorbate as the reducing substrate. The electron transfer from ascorbate to the type-1 copper center can be even faster and is completed within the dead time of the stopped-flow instrument. It is therefore not the rate limiting step in the overall reaction.

The factors governing electron transfer may be described within the framework of the Marcus electron-transfer theory (175). They are expressed in terms of driving force, distance of redox centers, reorganization energy, etc.

The driving force, calculated from the difference in the redox potentials (+344 mV for the type-1 copper in ascorbate oxidase (see Table VII); +295 mV for the couple ascorbate/ascorbate-free radical (176)) is 49 mV. In the proposed modeled encounter complex (74), there is a short distance of about 7 Å between the two redox centers (distance CU1—O1 ASC = 6.8 Å; distance CU1—O2 ASC = 7.5 Å) and an effective parallel arrangement of the rings, with good overlap of the π -electron density systems facilitating a rapid electron transfer (see Fig. 15).

It is well documented for small blue copper proteins, such as plastocyanin, that there are minimal structural changes upon reduction and reoxidation (160). The reorganization energy is, therefore, probably small.

B. INTRAMOLECULAR ELECTRON TRANSFER FROM THE TYPE-1 COPPER CENTER TO THE TRINUCLEAR COPPER CENTER

Long-distance intramolecular electron transfer can be described in the framework of the Marcus theory (175). In the formulation of Lieber *et al.* (177), the intramolecular electron rate constant, k_{ET} , can be written as

$$k_{ET} = \nu_n \Gamma \exp(-\Delta G^*/RT), \quad (1)$$

where ν_n is the nuclear frequency factor, normally 10^{13} sec^{-1} , Γ is the electronic factor, and ΔG^* is the activation free energy for ET. The electronic factor, Γ , is at unity when the donor and acceptor are strongly coupled but is much smaller at long donor-acceptor distances. In such cases, Γ is expected to fall off with distance, d ,

$$\Gamma = \Gamma(d_0) \exp[-\beta(d - d_0)], \quad (2)$$

where d_0 is the van der Waals contact distance, normally taken as 3 Å (175), and β is the electron coupling factor, which decreases with increasing distance and depends on the nature of the intervening medium. ΔG^* depends on the reaction free energy, ΔG° , and the nuclear

reorganization energy, λ (175), according to the equation

$$\Delta G^* = (\Delta G^\circ + \lambda)^2/4\lambda. \quad (3)$$

The ET rate is maximal when $-\Delta G^\circ = \lambda$.

The shortest distances, d , between the type-1 copper and the coppers of the trinuclear copper site are 12.2 Å (CU1 K1—CU2 K3) and about 12.7 Å (CU1 K1—CU3 K3) (see Table III). Figure 7 shows that His-506—Cys507—His508 serves as a bridging ligand between the two redox centers, providing a bifurcated pathway for ET from the type-1 copper center to the trinuclear copper species. The difference in the redox potential of the type-1 copper center and that of the type-3 coppers, the driving force, measured at 10°C, is $-\Delta G^\circ = 30$ mV (18). However, the binding of dioxygen to the partly reduced protein and the presence of reduction intermediates may affect this redox potential (a very slow equilibration was found between type-1 and type-3 coppers in ascorbate oxidase in the absence of dioxygen (178)). For the reorganization energy, λ , and the electronic coupling factor, β , no estimates can be derived for ascorbate oxidase but reasonable values for proteins are $\lambda = 1$ eV and $\beta = 1.2$ Å⁻¹, according to Gray and Malmström (179). These values inserted into Eq. (1) yield $k_{\text{ET}} \sim 10^5$ sec⁻¹. Changing β to 1.6 Å⁻¹ gives $k_{\text{ET}} \sim 4 \times 10^3$ sec⁻¹, a value closer to the observed turnover number of 8×10^3 sec⁻¹.

It has been suggested that the electron transfer in proteins may not be designed for very fast intramolecular ET, with the exception of light-induced ET in photosynthetic reaction centers (180). They could even be designed to slow down these rapid rates, which might otherwise lead to biological "short circuits." Related to this point is the observation that maximal rates for intramolecular ET in organic donor-acceptor molecules with rigid spacers are significantly faster than those for Ru-labeled protein systems at similar distances (181).

In the case of laccase and ascorbate oxidase, the observed ET rates for the reduction of the type-3 coppers (see Table VIII) are lower than the observed turnover number. This can be explained only by the possibility that the enzymes are in a resting form under the experimental conditions. A considerable reorganization energy seems to be necessary to get to the reduced state of the type-3 coppers (release of the bridging OH⁻ and movement of the copper CU2 and CU3). From these data it cannot be decided what the rate-limiting step is in the catalytic cycle, either this intramolecular ET or the reaction of the dioxygen at the trinuclear copper site.

ET from the type-1 copper to the type-3 copper pair of the trinuclear copper site may be through-bond, through-space, or a combination of both. A through-bond pathway is available for both branches, each with 11 bonds (see Fig. 7). The alternative combined through-bond and through-space pathway from the type-1 copper CU1 K1 to CU2 K3 of the trinuclear center involves a transfer from the SG atom of Cys507 to the main-chain carbonyl of Cys507 and through the hydrogen bond of this carbonyl to the ND1 atom of the His506.

Kyritsis *et al.* (129) carried out a theoretical pathway analysis for ascorbate oxidase using an algorithm, which was developed by Beratan and Onuchic (182–184) to help identify the most favorable long-range electron transfer pathways in metalloproteins. According to this analysis, the most favored route consists of four covalent bonds and a hydrogen bond between main-chain carbonyl O of Cys507 and the ND1 atom of His506 (hydrogen bond length, 2.9 Å) (see Fig. 7, which gives an electronic coupling ϵ^2 value of 2.3×10^{-3}). The second most efficient pathway contains an extra covalent bond between the ND1 and the CG atoms of His506, and gives an ϵ^2 value of 8.3×10^{-4} . For the second imidazole ring the best pathway consists of seven covalent bonds between SG of Cys507 and CG of His508, with an ϵ^2 value of 7.8×10^{-4} . Thus the hydrogen-bonded Cys507–His506 pathway gives approximately three times more efficient electronic coupling than the Cys507–His508 route. In the case of the type-1 blue copper protein plastocyanin, it is believed that a similar electron-transfer pathway, consisting of the copper ligand Cys84 and the adjacent highly conserved Tyr83 is relevant and made use of in the reaction with cytochrome *f* (185).

C. ELECTRON TRANSFER WITHIN THE TRINUCLEAR COPPER SITE

Electron exchange within the trinuclear copper site is expected to be very fast due to the short distances between the copper atoms (from 3.7 to 5.2 Å in the reduced form), as is ET to the bound dioxygen. This fast electron exchange is necessary to include CU4 into the redox processes. CU4 is at a greater distance from the type-1 copper CU1 than from CU2 and CU3.

XIII. Summary

It was the aim of this chapter to demonstrate the progress in the field of the blue-copper-containing oxidases during the last 10 years.

This progress is mainly due to the determination of the amino-acid sequences for all members of this group and the X-ray crystal structure of ascorbate oxidase. The three-dimensional structure of ascorbate oxidase showed the nature and spatial arrangement of the copper centers and the three-domain structure. However, modern spectroscopic techniques (e.g., low-temperature MCD and ENDOR) made invaluable contributions as well.

A structurally based amino-acid sequence alignment strongly suggests a three-domain structure for laccase, closely related to ascorbate oxidase, and a six-domain structure for ceruloplasmin. These domains demonstrate homology with the small blue copper proteins. The relationship suggests that laccase, like ascorbate oxidase, has a mononuclear blue copper in domain 3 and a trinuclear copper between domain 1 and domain 3, and ceruloplasmin has mononuclear copper ions in domains 2, 4, and 6 and a trinuclear copper between domain 1 and domain 6.

X-ray structures of functional derivatives of ascorbate oxidase provided pictures of intermediate states, which will probably be passed during the catalytic cycle. A catalytic mechanism that is based on the available mechanistic data and these new results has been proposed.

ACKNOWLEDGMENTS

The author thanks Professors R. Huber and R. Ladenstein and other colleagues involved in the X-ray structural work on ascorbate oxidase. These results would not have been possible without their expertise, cooperation, and support. Furthermore, he is indebted to Professor E. Adman for supplying the coordinates of nitrite reductase prior to their being deposited in the data bank.

REFERENCES

1. King, T. E., Mason, H. S., and Morrison, M., eds., *Prog. Clin. Biol. Res.* **274**, 1 (1988).
2. Capaldi, R. A., *Annu. Rev. Biochem.* **59**, 569 (1990).
3. Malkin, R., and Malmström, B. G., *Adv. Enzymol.* **33**, 177 (1970).
4. Yoshida, H., *J. Chem. Soc. Jpn.* **43**, 472 (1883).
5. Bertrand, G., *C.R. Hebd. Seances Acad. Sci.* **118**, 1215 (1894).
6. Keilin, D., and Mann, T., *Nature (London)* **143**, 23 (1939).
7. Malmström, B. G., Andreasson, L.-E., and Reinhammar, B., in "The Enzymes" (P. D. Boyer, ed.), Vol. 12B, pp. 507–579. Academic Press, New York, 1975.
8. Fee, J. A., *Struct. Bonding (Berlin)* **23**, 1 (1975).
9. Reinhammar, B., and Malmström, B. G., in "Copper Proteins, Metal Ions in Biology" (T. G. Spiro, ed.), Vol. 3, pp. 109–149. Wiley & Sons, New York, 1981.

10. Reinhammar, B., in "Copper Proteins and Copper Enzymes" (R. Lontie, ed.), Vol. 3, pp. 1-35. CRC Press, Boca Raton, FL, 1984.
11. Farver, O., and Pecht, I., in "Copper Proteins and Copper Enzymes" (R. Lontie, ed.), Vol. 1, pp. 183-214. CRC Press, Boca Raton, FL, 1984.
12. Mayer, A. M., *Phytochemistry* **26**, 11 (1987).
13. Szent-Györgyi, A., *Biochem. J.* **22**, 1387 (1928).
14. Szent-Györgyi, A., *Science* **72**, 125 (1930).
15. Lovett-Janison, P. L., and Nelson, J. M., *J. Am. Chem. Soc.* **62**, 1409 (1940).
16. Stotz, E., *J. Biol. Chem.* **133**, 69 (1940).
17. Dawson, C. R., in "The Biochemistry of Copper" (J. Peisach, P. Aisen, and W. E. Blumberg, eds.), pp. 305-337. Academic Press, New York, 1966.
18. Kroneck, P. M. H., Armstrong, F. A., Merkle, H., and Marchesini, A., *Adv. Chem. Ser.* **200**, 223-248 (1982).
19. Mondovi, B., and Avigliano, L., in "Copper Proteins and Copper Enzymes" (R. Lontie, ed.), Vol. 3, pp. 101-118. CRC Press, Boca Raton, FL, 1984.
20. Finazzi-Agro, A., *Life Chem. Rep.* **5**, 199 (1987).
21. Holmberg, C. G., *Acta Physiol. Scand.* **8**, 227 (1944).
22. Holmberg, C. G., and Laurell, C.-B., *Scand. J. Lab. Clin. Invest.* **3**, 103 (1951).
23. Malmström, B. G., and Rydén, L., in "Biological Oxidations" (T. Singer, ed.), pp. 415-438. Wiley, New York, 1968.
24. Poulik, M. D., and Weiss, M. L., in "The Plasma Proteins" (F. W. Putnam, ed.), Vol. 2, pp. 51-108. Academic Press, New York, 1975.
25. Frieden, E., and Hsieh, H. S., *Adv. Enzymol.* **44**, 187 (1976).
26. Rydén, L., in "Copper Proteins and Copper Enzymes" (R. Lontie, ed.), Vol. 3, pp. 37-100. CRC Press, Boca Raton, FL, 1984.
27. Laurie, S. H., and Mohammed, E. S., *Coord. Chem. Rev.* **33**, 279 (1980).
28. Cousins, R. J., *Physiol. Rev.* **65**, 238 (1985).
29. Arnaud, P., Gianazza, E., and Miribel, L., in "Methods in Enzymology" (G. D. Sabato, ed.), Vol. 163, p. 441. Academic Press, San Diego, 1988.
30. Mayer, A. M., *Phytochemistry* **26**, 11 (1987).
31. Pachlewski, R., and Crusciak, E., *Acta Mycol.* **16**, 97 (1980).
32. Saloheimo, M., Niku-Paalova, M.-L., and Knowles, J. K. C., *J. Gen. Microbiol.* **137**, 1537 (1991).
33. Rehmann, A. U., and Thurston, C. F., *J. Gen. Microbiol.* **138**, 1251 (1992).
34. Froehner, S. C., and Eriksson, K.-E., *J. Bacteriol.* **120**, 458 (1974).
35. Lerch, K., Deinum, J., and Reinhammar, B., *Biochim. Biophys. Acta* **534**, 7 (1978).
36. Thakker, G. D., Evans, C. S., and Rao, K. K., *Appl. Microbiol. Biotechnol.* **37**, 321 (1992).
37. Choi, G. H., Larson, T. G., and Nuss, D. I., *Mol. Plant-Microbe Interact.* **5**, 119 (1992).
38. Law, C. J., and Timberlake, W. E., *J. Bacteriol.* **144**, 509 (1980).
39. Germann, U. A., Müller, G., Hunziker, P. E., and Lerch, K., *J. Biol. Chem.* **263**, 885 (1988).
40. Aramayo, R., and Timberlake, W. E., *Nucleic Acids Res.* **18**, 3415 (1990).
41. Kosima, Y., Tsukuda, Y., Kawai, Y., Tsukamoto, A., Sugiura, J., Sakaino, M., and Kita, Y., *J. Biol. Chem.* **265**, 15,224 (1990).
42. Leatham, G. F., and Stahmann, M. A., *J. Gen. Microbiol.* **125**, 147 (1981).
43. Leonhard, T. J., *J. Bacteriol.* **106**, 162 (1971).
44. Clutterbuck, A. J., *J. Gen. Microbiol.* **70**, 423 (1972).
45. Ander, P., and Eriksson, K.-E., *Arch. Microbiol.* **109**, 1 (1976).

46. Kirk, T. K., and Shimada, M., in "Biosynthesis and Biodegradation of Wood Compounds" (T. Higuchi, ed.), pp. 579–605. Academic Press, San Diego, 1985.
47. Marbach, I., Hard, E., and Mayer, A. M., *Phytochemistry* **24**, 2559 (1985).
48. Geiger, J.-P., Nicole, M., Nandris, D., and Rio, B., *Eur. J. Pathol.* **16**, 22 (1986).
49. Saloheimo, M., and Niku-Paalova, M.-L., *Bio Technology* **9**, 987 (1991).
50. Chichiricco, G., Ceru, M. P., D'Alessandro, A., Oratore, A., and Avigliano, L., *Plant Sci.* **64**, 61 (1989).
51. Ohkawa, J., Okada, N., Shinmyo, A., and Takano, M., *Proc. Natl. Acad. Sci. U.S.A.* **86**, 1239 (1989).
52. Esaka, M., Hattori, T., Fujisawa, K., Sakajo, S., and Asahi, T., *Eur. J. Biochem.* **191**, 537 (1990).
53. Rossi, A., Petruzzelli, R., Messerschmidt, A., and Finazzi-Agro, A., private communication (1991).
54. Marchesini, A., Cappalletti, P., Canonica, L., Danieli, B., and Tollari, S., *Biochim. Biophys. Acta* **484**, 290 (1977).
55. Butt, V. S., in "The Biochemistry of Plants" (R. Davies, ed.), pp. 85–95. Academic Press, New York, 1980.
56. Lin, L.-S., and Varner, J. E., *Plant Physiol.* **96**, 159 (1991).
- 56a. "Biochemical Catalogue," p. 108. Boehringer Mannheim, 1991.
57. Takahashi, N., Ortel, T. L., and Putnam, F. W., *Proc. Natl. Acad. Sci. U.S.A.* **81**, 390 (1984).
58. Koschinsky, M. L., Funk, W. D., van Oost, B. A., and MacGillivray, R. T. A., *Proc. Natl. Acad. Sci. U.S.A.* **85**, 5086 (1986).
59. Fleming, R. E., and Gitlin, J. D., *J. Biol. Chem.* **265**, 7701 (1990).
60. Cooper, E., and Ward, M., *Invest. Cell Pathol.* **2**, 293 (1979).
61. Gitlin, D., and Gitlin, J. D., in "The Plasma Proteins" (F. W. Putnam, ed.), Vol. 2, pp. 321–374. Academic Press, New York, 1975.
62. Fahraeus, G., and Reinhammar, B., *Acta Chem. Scand.* **21**, 2367 (1967).
63. Mosbach, R., *Biochim. Biophys. Acta* **73**, 204 (1963).
64. Briving, C., *Ph.D. Thesis, University of Göteborg*, Göteborg, Sweden (1975).
65. Niku-Paalova, M.-L., Karhunen, E., Salola, P., and Raumio, V., *Biochem. J.* **254**, 877 (1988).
66. Reinhammar, B., *Biochim. Biophys. Acta* **205**, 35 (1970).
67. Marchesini, A., and Kroneck, P. M. H., *Eur. J. Biochem.* **101**, 65 (1979).
68. D'Andrea, G., Bowstra, J. B., Kamerling, J. P., and Vliegenthart, J. F. G., *Glycoconjugate* **5**, 151 (1988).
69. Nakamura, T., Makino, N., and Ogura, Y., *J. Biochem. (Tokyo)* **64**, 189 (1968).
70. Karhunen, E., Niku-Paalova, M.-L., Viikari, L., Haltia, T., van der Meer, R. A., and Duine, J. A., *FEBS Lett.* **267**, 6 (1990).
71. Kawahara, K., Suzuki, S., Sakurai, T., and Nakahara, A., *Arch. Biochem. Biophys.* **241**, 179 (1985).
72. Sakurai, T., Suzuki, S., and Tanabe, Y., *Inorg. Chim. Acta* **157**, 117 (1989).
73. Messerschmidt, A., Rossi, A., Ladenstein, R., Huber, R., Bolognesi, M., Gatti, G., Marchesini, A., Petruzzelli, R., and Finazzi-Agro, A., *J. Mol. Biol.* **206**, 513 (1989).
74. Messerschmidt, A., Ladenstein, R., Huber, R., Bolognesi, M., Avigliano, L., Petruzzelli, R., Rossi, A., and Finazzi-Agro, A., *J. Mol. Biol.* **224**, 179 (1992).
75. Bränden, R., and Deinum, J., *FEBS Lett.* **73**, 144 (1977).
76. Martin, C. T., Morse, R. H., Kanne, R. M., Gray, H. B., Malmström, B. G., and Chan, S. I., *Biochemistry* **20**, 5147 (1981).

77. Morpurgo, L., Desideri, A., and Rotilio, G., *Biochem. J.* **207**, 625 (1982).
78. Winkler, M. E., Spira, D. J., LuBien, C. D., Thamann, T. J., and Solomon, E. I., *Biochem. Biophys. Res. Commun.* **107**, 727 (1982).
79. Allendorf, M. D., Spira, D. J., and Solomon, E. I., *Proc. Natl. Acad. Sci. U.S.A.* **82**, 3063 (1985).
80. Spira-Solomon, D. J., Allendorf, M. D., and Solomon, E. I., *J. Am. Chem. Soc.* **108**, 5318 (1986).
81. Deutsch, H. F., Kasper, C. B., and Walsh, D. E., *Arch. Biochem. Biophys.* **99**, 132 (1962).
82. Magdoff-Fairchild, B., Lovell, F. M., and Low, B. W., *J. Biol. Chem.* **244**, 3497 (1969).
83. Zaytsev, V. N., Moshkov, K. A., Shavlovski, M. M., and Neifakh, S. A., *Bioorg. Khim.* **1**, 1521 (1975).
84. Zaytsev, V. N., Vagin, A. A., Nekrasov, Yu., V., and Moshkov, K. A., *Kristallografiya* **31**, 937 (1986).
85. Ladenstein, R., Marchesini, A., and Palmieri, S., *FEBS Lett.* **107**, 407 (1979).
86. Bolognesi, M., Gatti, G., Coda, A., Avigliano, L., Marcozzi, G., and Finazzi-Agro, A., *J. Mol. Biol.* **169**, 351 (1983).
87. Priestle, J. P., *J. Appl. Crystallogr.* **21**, 572 (1988).
88. Kabsch, W., and Sander, S., *Biopolymers* **22**, 2577 (1983).
89. Barlow, D. J., and Thornton, J. M., *J. Mol. Biol.* **168**, 867 (1983).
90. Crawford, J. L., Lipscomb, W. N., and Schellmann, C. C., *Proc. Natl. Acad. Sci. U.S.A.* **70**, 538 (1973).
91. Richardson, J. S., *Adv. Protein Chem.* **34**, 167 (1981).
92. Huber, R., and Steigemann, W., *FEBS Lett.* **48**, 235 (1974).
93. Baker, E. N., and Hubbard, R. E., *Prog. Biophys. Mol. Biol.* **44**, 97 (1984).
94. Lee, B. K., and Richards, F. M., *J. Mol. Biol.* **55**, 379 (1971).
95. Guss, J. M., and Freeman, H. C., *J. Mol. Biol.* **169**, 521 (1983).
96. Nar, H., Messerschmidt, A., Huber, R., van de Kamp, M., and Canters, G. W., *J. Mol. Biol.* **221**, 765 (1991).
97. Cole, J. L., Clark, P. A., and Solomon, E. I., *J. Am. Chem. Soc.* **112**, 9534 (1990).
98. Karlin, K. D., Hayes, J. C., Gultneh, Y., Cruse, R. W., McKnown, J. W., Hutchinson, J. P., and Zubietta, J., *J. Am. Chem. Soc.* **106**, 2121 (1984).
99. Chaudhuri, P., Venter, D., Wieghardt, K., Peters, E., Peters, K., and Simon, A., *Angew. Chem.* **97**, 55 (1985).
100. Volbeda, A., and Hol, W. G. J., *J. Mol. Biol.* **209**, 249 (1989).
101. Messerschmidt, A., and Huber, R., *Eur. J. Biochem.* **187**, 341 (1990).
102. Vehar, G. A., Key, B., Eaton, D., Rodriguez, H., O'Brien, D. P., Rotblat, F., Oppermann, H., Keck, R., Wood, W. I., Harkins, R. N., Tuddenham, E. G. D., Lawn, R. M., and Capon, D. J., *Nature (London)* **312**, 337 (1984).
103. Kane, W. H., and Davie, E. W., *Proc. Natl. Acad. Sci. U.S.A.* **83**, 6800 (1986).
104. Karlsson, G., Aasa, R., Malmström, B. G., and Lundberg, L. G., *FEBS Lett.* **253**, 99 (1989).
105. Deinum, J., and Vänngård, T., *Biochim. Biophys. Acta* **310**, 321 (1973).
106. Carrica, R. J., Malmström, B. G., and Vänngård, T., *Eur. J. Biochem.* **22**, 127 (1971).
107. Ortel, T. L., Takahashi, N., and Putnam, F. W., *Proc. Natl. Acad. Sci. U.S.A.* **81**, 4761 (1984).
108. Moshkov, K. A., Vagin, A. A., and Zaytsev, V. N., *Mol. Biol. (Moscow)* **21**, 1124 (1987).
109. Rydén, L., *Proc. Natl. Acad. Sci. U.S.A.* **79**, 6767 (1982).

110. Godden, J. W., Turley, S., Teller, D. C., Adman, E. T., Liu, M. Y., Payne, W. J., and LeGall, J., *Science* **258**, 438 (1991).
111. Fenderson, F. F., Kumar, S., Adman, E. T., Liu, M.-Y., Payne, W. J., and LeGall, J., *Biochemistry* **30**, 7180 (1991).
112. Adman, E. T., *Adv. Protein Chem.* **42**, 145 (1991).
113. Villafranca, F. F., Freeman, F. C., and Kotcherar, A., in "Bioinorganic Chemistry of Copper" (K. D. Karlin and Z. Tyeklar, eds.), pp. 439–446. Chapman and Hall, New York, 1993.
114. Barry, C. E., Nayar, P. G., and Begley, T. P., *Biochemistry* **28**, 6323 (1989).
115. Mellano, M. A., and Cooksey, D. A., *J. Bacteriol.* **170**, 2879 (1988).
116. Albani, D., Sardana, R., Robert, L. S., Altosaar, I., Arnison, P. G., and Fabijanski, S. F., *Plant J.* **2**, 331 (1992).
117. Dwulet, F. E., and Putnam, F. W., *Proc. Natl. Acad. Sci. U.S.A.* **78**, 2805 (1981).
118. Rydén, L., in "Oxidases and Related Redox Systems" (T. S. King, H. S. Mason, and M. Morrison, eds.), pp. 349–366. Alan R. Liss, New York, 1988.
119. George, D. G., "Multiple Sequence Alignment Program ALNED." NBRF, Washington, DC, 1988.
120. Reinhammar, B., *Biochim. Biophys. Acta* **275**, 245 (1972).
121. Reimhammar, B., and Vänngard, T., *Eur. J. Biochem.* **18**, 463 (1971).
122. Sykes, A. G., *Adv. Inorg. Chem.* **36**, 377 (1991).
123. Peterson, L. C., and Degn, H., *Biochim. Biophys. Acta* **526**, 85 (1978).
124. Andreasson, L.-E., and Reinhammar, B., *Biochim. Biophys. Acta* **445**, 579 (1976).
125. Andreasson, L.-E., Malmström, B. G., Stromberg, C., and Vänngard, T., *Eur. J. Biochem.* **34**, 434 (1973).
126. O'Neill, P., Fielden, E. M., Morpurgo, L., and Agostinelli, E., *Biochem. J.* **222**, 71 (1984).
127. O'Neill, P., Fielden, E. M., Finazzi-Agro, A., and Avigliano, L., *Biochem. J.* **209**, 167 (1983).
128. Meyer, T. E., Marchesini, A., Cusanovich, M. A., and Tollin, G., *Biochemistry* **30**, 4619 (1991).
129. Kyritsis, P., Messerschmidt, A., Huber, R., Salmon, G. A., and Sykes, A. G., *J. Chem. Soc., Dalton Trans.* 73 (1992).
130. Farver, O., and Pecht, I., *Proc. Natl. Acad. Sci. U.S.A.* **89**, 8283 (1992).
131. Yamazaki, I., and Piette, L. H., *Biochim. Biophys. Acta* **50**, 62 (1961).
132. Farver, O., and Pecht, I., *Mol. Cryst. Liq. Cryst.* **194**, 215 (1991).
133. Andreasson, L.-E., and Reinhammar, B., *Biochim. Biophys. Acta* **568**, 145 (1979).
134. Andreasson, L.-E., Bränden, R., and Reinhammar, B., *Biochim. Biophys. Acta* **438**, 370 (1976).
135. Nakamura, T., and Ogawa, Y., *J. Biochem. (Tokyo)* **64**, 267 (1968).
136. Farver, O., Goldberg, M., and Pecht, I., *FEBS Lett.* **94**, 383 (1978).
137. Strothkamp, R. E., and Dawson, C. R., *Biochem. Biophys. Res. Commun.* **85**, 655 (1978).
138. Cole, J. L., Ballou, D. P., and Solomon, E. I., *J. Am. Chem. Soc.* **113**, 8544 (1991).
139. Clark, P. A., and Solomon, E. I., *J. Am. Chem. Soc.* **114**, 1108 (1992).
140. Curzon, G., *Biochem. J.* **100**, 295 (1966).
141. Curzon, G., and Speyer, B. E., *Biochem. J.* **105**, 243 (1967).
142. Gunnarsson, P.-O., Nylén, U., and Pettersson, G., *Eur. J. Biochem.* **27**, 572 (1972).
143. Gunnarsson, P.-O., and Pettersson, G., *Eur. J. Biochem.* **27**, 564 (1972).
144. Malkin, R., Malmström, B. G., and Vänngard, T., *FEBS Lett.* **1**, 50 (1968).

145. Bränden, R., Mamström, B. G., and Vänngard, T., *Eur. J. Biochem.* **36**, 195 (1973).
146. Strothkamp, R. E., and Dawson, C. R., *Biochemistry* **16**, 1926 (1977).
147. van Leeuwen, F. X. R., Wever, R., van Gelder, B. F., Avigliano, L., and Mondovi, B., *Biochim. Biophys. Acta* **285**, 285 (1975).
148. Morie-Bebel, M. M., Morris, M. C., Menzie, J. L., and McMillin, D. R., *J. Am. Chem. Soc.* **106**, 3677 (1984).
149. Messerschmidt, A., Steigemann, W., Huber, R., Lang, G., and Kroneck, P. M. H., *Eur. J. Biochem.* **209**, 597 (1992).
150. Messerschmidt, A., Luecke, H., and Huber, R., *J. Mol. Biol.* **230**, 997 (1993).
151. Malkin, R., Malmström, B. G., and Vänngard, T., *Eur. J. Biochem.* **7**, 253 (1969).
152. Hanna, P. H., McMillin, D. R., Pasenkiewicz-Gierula, M., Antholine, W. E., and Reinhammar, B., *Biochem. J.* **253**, 561 (1988).
153. Graziani, M. T., Morpurgo, L., Rotilio, G., and Mondovi, B., *FEBS Lett.* **70**, 87 (1976).
154. Reinhammar, B., and Oda, Y., *J. Inorg. Biochem.* **11**, 115 (1979).
155. Schmidt-Klemens, A., and McMillin, D. R., *J. Inorg. Biochem.* **38**, 107 (1990).
156. Graziani, M. T., Loreti, P., Morpurgo, L., Savini, I., and Avigliano, L., *Inorg. Chim. Acta* **173**, 261 (1990).
157. Avigliano, L., Desideri, A., Urbanelli, S., Mondovi, B., and Marchesini, A., *FEBS Lett.* **100**, 318 (1979).
158. Morpurgo, L., Savini, I., Mondovi, B., and Avigliano, L., *J. Inorg. Biochem.* **29**, 25 (1987).
159. Merli, A., Rossi, G. L., Bolognesi, M., Gatti, G., Morpurgo, L., and Finazzi-Agro, A., *FEBS Lett.* **231**, 89 (1988).
160. Guss, J. M., Harrowell, P. R., Murata, M., Norris, V. A., and Freeman, H. C., *J. Mol. Biol.* **192**, 361 (1986).
161. Shepard, W. E. B., Anderson, B. F., Lewandowski, D. H., Norris, G. E., and Baker, E. N., *J. Am. Chem. Soc.* **112**, 7817 (1990).
162. Nar, H., Ph.D. Thesis, Technische Universität München (1992).
163. Schilstra, M. J., Birker, P. J. M. W., Verschoor, G. C., and Reedijk, J., *J. Inorg. Chem.* **21**, 2631 (1982).
164. Sorell, T. N., and Malachowski, M. R., *Inorg. Chem.* **22**, 1883 (1983).
165. Kitajima, N., Fujisawa, K., and Moro-oka, Y., *J. Am. Chem. Soc.* **111**, 8975 (1989).
166. Magnus, K., and Ton-That, H., *J. Inorg. Biochem.* **47**, 20 (1992).
167. Andreasson, L.-E., Bränden, R., Malmström, B. G., and Vänngard, T., *FEBS Lett.* **32**, 187 (1973).
168. Aasa, R., Bränden, R., Deinum, J., Malmström, B. G., Reimhammar, B., and Vänngard, T., *FEBS Lett.* **61**, 115 (1976).
169. Aasa, R., Bränden, R., Deinum, J., Malmström, B. G., Reimhammar, B., and Vänngard, T., *Biochem. Biophys. Res. Commun.* **70**, 1204 (1976).
170. Bränden, R., and Deinum, J., *Biochim. Biophys. Acta* **524**, 297 (1978).
171. Cole, J. L., Avigliano, L., Morpurgo, L., and Solomon, E. I., *J. Am. Chem. Soc.* **113**, 9080 (1991).
172. Casella, L., Gullotti, M., Pallanza, G., Pintar, A., and Marchesini, A., *Biochem. J.* **251**, 441 (1988).
173. Casella, L., Gullotti, M., Pintar, A., Pallanza, G., and Marchesini, A., *J. Inorg. Biochem.* **37**, 105 (1989).
174. Hathaway, B. J., *Compr. Coord. Chem.* **5** (1987).
175. Marcus, R. A., and Sutin, N., *Biochim. Biophys. Acta* **811**, 265 (1985).
176. Farver, O., Goldberg, M., Wherland, S., and Pecht, I., *Proc. Natl. Acad. Sci. U.S.A.* **75**, 5245 (1978).

177. Lieber, C. M., Karas, J. L., Mayo, S. L., Albin, M., and Gray, H. B., in "Proceedings of the Robert A. Welsh Conference on Chemical Research. Design of Enzymes and Enzyme Model," pp. 9–33. Robert A. Welsh Found., Houston, TX, 1987.
178. Avigliano, L., Rotilio, G., Urbanelli, S., Mondovi, B., and Finazzi-Agro, A., *Arch. Biochem. Biophys.* **185**, 419 (1978).
179. Gray, H. B., and Malmström, B. G., *Biochemistry* **28**, 7499 (1989).
180. McLendon, G., *Acc. Chem. Res.* **21**, 160 (1988).
181. Mayo, S. L., Ellis, W. R., Jr., Crutchley, R. J., and Gray, H. B., *Science* **233**, 948 (1986).
182. Onuchic, J. N., and Beratan, D. N., *J. Chem. Phys.* **92**, 722 (1990).
183. Beratan, D. N., Onuchic, J. N., and Gray, H. B., in "Metal Ions in Biological Systems" (H. Sigel and A. Sigel, eds.), pp. 97–127. Dekker, New York, 1991.
184. Beratan, D. N., Onuchic, J. N., Betts, J. N., Bowler, B., and Gray, H. B., *J. Am. Chem. Soc.* **112**, 7915 (1990).
185. Sykes, A. G., *Struct. Bonding (Berlin)* **75**, 175 (1991).